Quantum chemical methods for high-energy materials – estimating formation enthalpies, crystal densities and impact sensitivities

Eirik Fadum Kjønstad

FFI Forsvarets
forskningsinstitutt

Quantum chemical methods for high-energy materials – estimating formation enthalpies, crystal densities and impact sensitivities

Eirik Fadum Kjønstad

Norwegian Defence Research Establishment (FFI)

15 December 2014

Keywords

Kvantekjemi

Krystalltetthet

Dannelsesentalpi

Følsomhet

Høy-energetiske forbindelser

Approved by

Ivar Sollien   Project Manager

Erik Unneberg   Research manager

Jon Skjervold   Director

English summary

A preliminary investigation of quantum chemical methods for the calculation of formation enthalpies, crystal densities, and impact sensitivities is presented. In particular, all calculations presented are density functional theory calculations with the B3LYP functional and the 6-31g(d) basis set. In total, 14 high-energy compounds were investigated, including the known RDX, NTO, and TNT, as well as some recently proposed compounds.

Gas formation enthalpies were calculated from atomization energies together with experimental element formation enthalpies. Solid formation enthalpies were obtained from those of gas phase by either experimental sublimation enthalpy data or empirical methods. The root mean square error for the evaluation of solid formation enthalpies was found to be about 55 kJ/mol.

Crystal densities were approximated by two quantum chemical analogues of the empirical volume additivity procedure, as suggested in the work of Rice et al. [1] and Politzer et al. [2]. In particular, estimates were obtained by calculating the molecular volume as that enclosed by a 0.001 electrons/bohr^3 isosurface of the electron density. A variant of this approach, taking into account the electrostatic potential, is also evaluated. The root mean square error for these methods was found to be 0.10 g/cm^3. It is argued that this error is still too high for effective estimation of detonation and combustion parameters.

A correlation between bond dissociation energies and impact sensitivities was obtained, based on experimental data of the compounds RDX, NTO, TNT, and a trinitropyrazole. In particular, the logarithm of the impact energy was shown to vary linearly with the bond dissociation energy of the weakest $X-NO_2$ bond divided by the electronic ground-state energy. Based on this correlation, estimated impact energies for eight of the other compounds are presented.

Sammendrag

Muligheten for estimering av formasjonsentalpier, krystalltettheter og gjennomslagssensitivitet ved hjelp av kvantekjemiske metoder presenteres. Alle beregninger ble gjort med tetthetsfunksjonalteori, der B3LYP-funksjonalen sammen med et 6-31g(d) basis-sett er benyttet. Totalt ble beregninger utført på 14 molekyler, inkludert de mer kjente RDX, NTO, TNT, i tillegg til nye foreslåtte forbindelser.

Gassformasjonsentalpier ble beregnet fra atomiseringsenergier og eksperimentelle atomentalpiformasjonsdata. Formasjonsentalpier for fast fase ble funnet fra gassformasjonsentalpiene ved hjelp av enten eksperimentelle sublimeringsentalpidata eller empiriske metoder. Gjennomsnittlig rot-avvik ble bestemt til omlag 55 kJ/mol.

Krystalltettheter ble estimert ved hjelp av to kvantekjemiske analoger til volumadditivitetmetoden, foreslått i arbeidene til Rice et al. [1] og Politzer et al. [2]. Molekylvolumet i disse metodene ble estimert som volumet begrenset av en 0.001 elektroner/bohr^3 isoflate til elektrontettheten. En variant av denne metoden, der det elektrostatiske potensial begrenset til isoflaten er en ekstra faktor, er også evaluert. Gjennomsnittlig rot-avvik ble bestemt til 0.10 g/cm^3. Det argumenteres for at denne feilen er for stor for effektiv estimering av detonasjons- og forbrenningsparametre.

En korrelasjon ble funnet mellom dissosiasjonsenergier og gjennomslagssensitiviteter, basert på eksperimentelle data for RDX, NTO, TNT og et trinitropyrazol. Mer spesifikt korrelerer logaritmen til gjennomslagsenergien med dissosiasjonsenergien til den svakeste $X-NO_2$-bindingen dividert på den elektroniske grunntilstandsenergien. Basert på denne korrelasjonen, presenteres estimat for gjennomslagsenergien til åtte av de andre forbindelsene.

Contents

List of Symbols

α, β, γ	Parameters of the Politzer method. See equation 2.37.
$\bar{M}_g$	Mean molar mass of gaseous products.
$\chi(\mathbf{r})$	Atomic orbital
Δ_{RMSE}	Root mean square deviation
Δ_{sgn}	Signed mean error
$\mathbf{r}$	Electronic coordinates. Depending on context, it refers either to the set of N electron coordinates $\{\mathbf{r}_1, \mathbf{r}_2, \ldots, \mathbf{r}_N\}$ or a single electron coordinate.
$\mathcal{V}(\mathbf{r})$	Electrostatic potential
$\boldsymbol{\nabla} E(\mathbf{R})$	The gradient of the potential energy surface $E(\mathbf{R})$.
$\mathscr{H}$	Hamiltonian operator
$\mathbf{G}(\mathbf{R})$	The Hessian of the potential energy surface $E(\mathbf{R})$.
κ	Rate constant.
$\mathbf{Q}, Q_i$	The set of normal modes and a particular normal mode, respectively.
$\mathcal{Q}, \mathscr{Q}$	The partition function and molecular partition function, respectively.
ν_i	Stoichiometric coefficients
$\mathbf{R}$	Nuclear coordinates. See $\mathbf{r}$.
Ψ, ψ	Time-dependent and time-independent wavefunction, respectively.
ψ_{elec}	Wavefunction that is a solution to the electronic Schrödinger equation (2.3).
ρ	Crystal density
σ_-^2, σ_+^2	Variance of negative and positive values of $\mathcal{V}(\mathbf{r})$, $\mathbf{r}$ restricted to the 0.001 electrons/bohr^3 isosurface, respectively.
E_h	Hartree energy unit
$\varphi(\mathbf{r})$	Molecular orbital
ξ	Confidence interval fraction. See Table 4.9.
ζ	Orbital exponent of Gaussian type orbitals.
c^*	Characteristic velocity

D	Detonation velocity
E	Energy
$E(\mathbf{R})$	Electronic ground-state energy for a given set of nuclear coordinates $\mathbf{R}$. Usually called the potential energy surface in the context of optimization.
$E_{\text{xc}}[n(\mathbf{r})]$	Exchange-correlation functional
$F[n(\mathbf{r})]$	Hohenberg-Kohn functional
f_i	Normal mode frequencies.
g	Acceleration of gravity (9.81m/s)
$g(E_i)$	Degeneracy of energy level E_i.
H	Enthalpy
h	Planck's constant
h_{50}, I_{50}	Impact sensitivity. Measured by height and energy at which 50% of samples initiate, respectively.
I_{sp}	Specific impulse
$J[n(\mathbf{r})]$	Coulomb interaction of the electron density $n(\mathbf{r})$ with itself.
k	Boltzmann's constant
M	Mass
$n(\mathbf{r})$	Electron density at the point $\mathbf{r}$
N, Z_N	Nuclei and their charge, respectively.
N_A	Avogadro's number
P	Detonation pressure
p	Pressure
Q_v	Heat of explosion
R	Universal gas constant
r	Reaction rate.
T	Temperature
T_m	Melting point
$T_s[n(\mathbf{r})]$	Kinetic energy of a non-interacting system of electrons.
V	Volume

List of Figures

List of Tables

1 Introduction

This report was written as a part of a summer internship at FFI, 2014. The purpose I had in mind while writing this report was two-fold. First, to provide a brief introduction to the field of quantum chemistry. The methods routinely used in the field are rarely black-box and hence a good grasp of the different theoretical aspects is helpful. This accounts for the extensive theory section, which covers both general material to introduce the reader to quantum chemistry as well as some recent research within the high-energy materials field. Second, to present the results we achieved during these three months. In particular, we present estimates of formation enthalpies, impact sensitivities, and crystal densities for a range of known and novel high-energy compounds. These are shown in Figure 1.1.
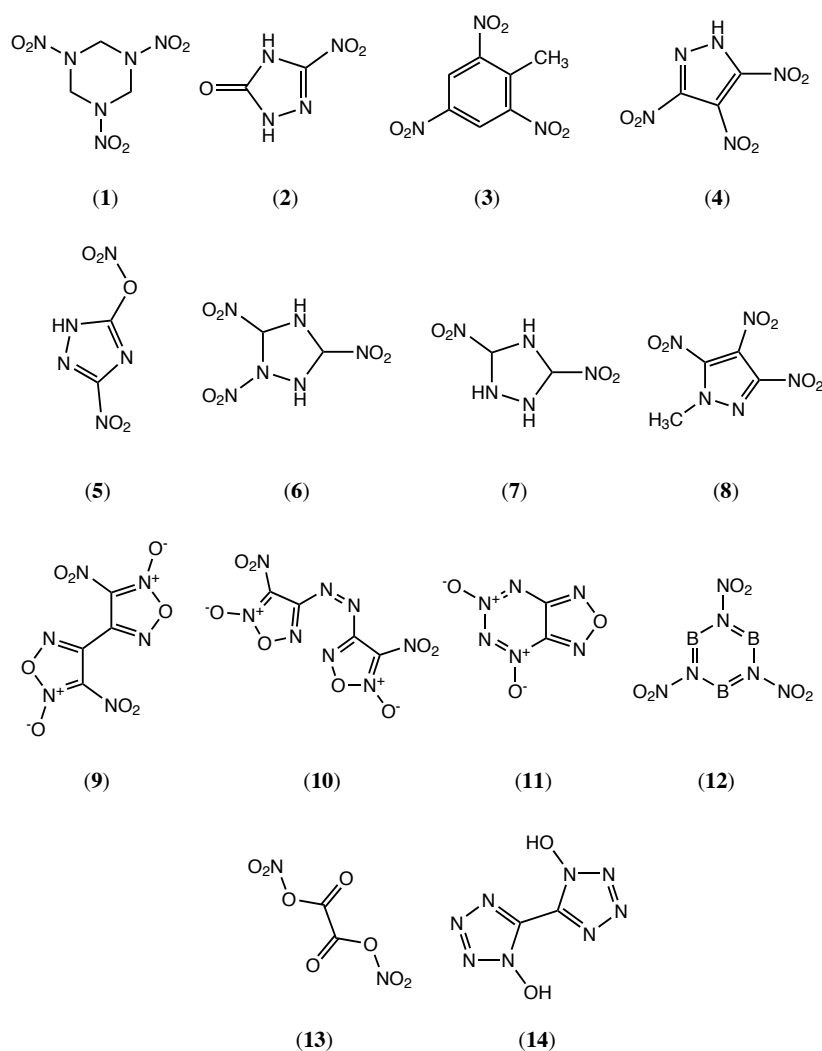
Figure 1.1   **Studied compounds**. RDX (**1**), NTO (**2**), TNT (**3**), a trinitropyrazole (**4**) [3], three alternatives to NTO (**5**, **6**, **7**) proposed by us, a compound studied by FOI (**8**) [4], three furazan derivatives (**9**, **10**, **11**) [5], a high-boron explosive (**12**) [6], a proposed alternative to ammonium perchlorate (**13**) [7], and a tetrazole (**14**) [7].

2 Theory

In quantum mechanics all the information one can possibly have of a system is encoded in the wavefunction Ψ. For time-independent problems, it is obtained by solving the *time-independent Schrödinger equation*

$$\mathscr{H}\psi = E\psi, \tag{2.1}$$

where $\mathscr{H}$ is the Hamilton operator, E is the energy, and ψ differs from Ψ by a phase-factor. For a given Hamiltonian, equation (2.1) can have many solutions, but normally we are most interested in the solution with the lowest energy E: the *ground-state* wavefunction and energy.

For molecular systems, the wavefunction will be a function of the electronic and nuclear coordinates, denoted $\mathbf{r}$ and $\mathbf{R}$, respectively. We write

$$\psi = \psi(\mathbf{r}, \mathbf{R}). \tag{2.2}$$

The Hamiltonian for such systems contains nuclear and electronic kinetic energy terms as well as Coulombic terms describing nuclear-nuclear repulsion, nuclear-electron attraction, and electron-electron repulsion.

Equation (2.1) is much too difficult to solve for molecular systems and one must resort to approximations. The first step is the decoupling of electronic and nuclear motion. The nuclei, being many times more massive than electrons, move slowly. Thus, from the point of view of electrons, the nuclei can be considered fixed. This is the *Born-Oppenheimer approximation* [8, 9]. For a given set of nuclear coordinates $\mathbf{R}$, one solves the *electronic Schrödinger equation*

$$\mathscr{H}\psi_{\text{elec}}(\mathbf{r}; \mathbf{R}) = E(\mathbf{R})\psi_{\text{elec}}(\mathbf{r}; \mathbf{R}). \tag{2.3}$$

The corresponding equation for the nuclei shows that they move in the potential energy generated by the electrons [9]; the function $E(\mathbf{R})$ is therefore sometimes called the *potential energy surface*. Methods that try to solve (2.3) directly are termed *ab initio* meaning "from first principles".

2.1 Geometry Optimization: Equilibrium Geometries and Transition Structures

The potential energy surface $E(\mathbf{R})$ describes the electronic energy of the system as the molecular geometry $\mathbf{R}$ changes. Stable conformations of a molecule correspond to minima of this potential energy and are called *equilibrium geometries*. A bond breaking, for example, can be described by movement from one minima $\mathbf{R}_{\text{reactants}}$ to another $\mathbf{R}_{\text{products}}$. During this *reaction path* the molecule reaches a point of highest potential energy called a *transition structure*[1]. In terms of the potential energy surface, transition structures are maxima in *one* direction and minima in all others: they are first order saddle points. Finding equilibrium geometries and transition structures is known as *geometry optimization*.

---

[1]Not to be confused with a *transition state*. The transition state may be different from the transition structure due to other contributions to the energy; e.g. it may be temperature-dependent [8].

Most optimization algorithms use information of inclination and curvature about a point $\mathbf{R}_k$ to select an appropriate step $\mathbf{R}_k \rightarrow \mathbf{R}_{k+1}$. This information is embodied in the gradient $\nabla E(\mathbf{R})$ and Hessian $\mathbf{G}(\mathbf{R})$ of E, respectively. The potential energy surface can be approximated by a Taylor expansion about some point $\mathbf{R}_k$, truncated after second order:

$$E(\mathbf{R}) = E(\mathbf{R}_k) + \nabla E(\mathbf{R}_k)(\mathbf{R} - \mathbf{R}_k) + \frac{1}{2}(\mathbf{R} - \mathbf{R}_k)^T \mathbf{G}(\mathbf{R}_k)(\mathbf{R} - \mathbf{R}_k). \tag{2.4}$$

Taking the gradient of this equation, and supposing that at $\mathbf{R}_{k+1}$ we will be at an extremum (i.e. $\nabla E(\mathbf{R}_{k+1}) = \mathbf{0}$), the *Newton-Raphson iteration* [10]

$$\mathbf{R}_{k+1} = \mathbf{R}_k - \mathbf{G}(\mathbf{R}_k)\nabla E(\mathbf{R}_k) \tag{2.5}$$

is obtained. Calculating and storing the Hessian $\mathbf{G}$ in each step is expensive, and optimization methods often approximate it. The *quasi-Newton methods*, for example, estimate $\mathbf{G}$ with increasing accuracy in each step [8]:

$$\lim_{l \to \infty} \mathbf{G}_l = \mathbf{G}. \tag{2.6}$$

The *GDIIS method*, which is the standard minimization method of the GAUSSIAN09 software, uses gradients and geometries of previous steps to minimize the Newton step $\mathbf{R}_{k+1} - \mathbf{R}_k$ [10]. The motivation for this can be appreciated by noting that, at convergence, the Newton step vanishes. For transition state searches another method is employed in GAUSSIAN09: *Rational function optimization* (RFO), for which the quadratic (2.4) is replaced by a rational function approximation [10, 11].

Not only is the Hessian indispensable for choosing the next step in optimizations, it also characterizes what kind of extremum has been found: if the Hessian $\mathbf{G}(\mathbf{R}^*)$ only has positive eigenvalues, then $\mathbf{R}^*$ is an equilibrium geometry; if it has *one* negative eigenvalue, $\mathbf{R}^*$ is a transition structure. We will return to transition structure searches in Section 2.9.

For a more detailed descriptions of these procedures, I recommend the review by Schlegel [10].

2.2 Electron-electron Interactions: Exchange and Correlation

One of the most challenging tasks in quantum chemistry is to properly describe the instantaneous interactions between electrons in a molecule. These interactions are normally grouped in two categories: *exchange* and *correlation*. According to the Pauli exclusion principle, no two electrons can be in the same quantum state [9]. Thus electrons tend to "avoid" one another; this purely quantum mechanical effect goes by the name of exchange. Correlation, on the other hand, refers to the more familiar instantaneous Coulombic interaction between electrons [12].

Which type of electron-electron interaction is dominant depends on the type of system. For transition structures, a particular type of correlation (called *static*) not present for equilibrium geometries becomes important. It arises from near-degeneracy of configurations as bonds are stretched[2]. This is not incorporated in *density functional theory* (DFT) [13], and is treated in

---

[2]This means that the determinants corresponding to the different configurations cannot be treated in isolation.

an *ad hoc* fashion by special functionals. For a proper description of such situations, *multi-reference* methods are needed [12].

Even though DFT requires different functionals for different applications, it combines high accuracy with low cost—comparable to Hartree-Fock—making it the ideal candidate for our investigations.

2.3 Density Functional Theory

Ab initio methods seek the wavefunction ψ by attempting to solve the electronic Schrödinger equation (2.3). Density functional theory, on the other hand, is based on the remarkable fact that ψ is not really needed: as shown by Hohenberg and Kohn [14], all the ground-state information of a system is determined solely by the *electron density* $n(\mathbf{r})$.

> **Definition 1** *The **electron density** $n(\mathbf{r})$ is the probability density to find an electron at $\mathbf{r}$.*

> **Theorem 1 (Hohenberg-Kohn existence theorem)** *The ground-state energy and all other ground-state electronic properties are uniquely determined by the electron density.*

Thus the ground-state energy is a function of the function $n(\mathbf{r})$, also known as a *functional*. We write $E = E[n(\mathbf{r})]$.

How does one decide if a given trial density $n'(\mathbf{r})$ is appropriate? A procedure is provided by the *DFT variation theorem* [9].

> **Theorem 2 (DFT variation theorem)** *For a trial density $n'(\mathbf{r})$, the calculated energy exceeds the ground-state energy of the true density $n(\mathbf{r})$. That is,*

$$E[n'(\mathbf{r})] \geq E[n(\mathbf{r})]. \tag{2.7}$$

It thus makes sense to choose the density which minimizes the energy.

The preceding discussion presupposes that the functional $E[n(\mathbf{r})]$ is known—this is *not* the case. To isolate contributions to the energy, it is common to introduce the *Hohenberg-Kohn functional* $F[n(\mathbf{r})]$, defined by

$$E[n(\mathbf{r})] = \underbrace{\int v(\mathbf{r})\, n(\mathbf{r})\, \mathrm{d}\mathbf{r}}_{\text{Electron-nuclear interaction}} + F[n(\mathbf{r})]. \tag{2.8}$$

The Hohenberg-Kohn functional is further divided into contributions to kinetic energy as well as correlation and exchange. A first approximation to the kinetic energy is provided by a non-interacting system of electrons and denoted $T_s[n(\mathbf{r})]$, while a first approximation to correlation is the Coulomb interaction $J[n(\mathbf{r})]$ of the electron density with itself. This *Kohn-Sham decomposition* of the energy serves to define the important *exchange-correlation functional* $E_{\mathrm{xc}}[n(\mathbf{r})]$:

$$F[n(\mathbf{r})] = T_s[n(\mathbf{r})] + J[n(\mathbf{r})] + E_{\mathrm{xc}}[n(\mathbf{r})]. \tag{2.9}$$

Note that DFT is only variational if the true functional $E[n(\mathbf{r})]$ is known. The variation theorem breaks down when an approximation of $E_{xc}[n(\mathbf{r})]$ is made.

To make use of this theory, a functional form of the density $n(\mathbf{r})$ is needed. The most common is the *Kohn-Sham approach* (KS), in which the density is written in terms of a set of functions called *molecular orbitals* φ_i:[3]

$$n_{KS}(\mathbf{r}) = \sum_i |\varphi_i(\mathbf{r})|^2 \tag{2.10}$$

Minimizing the energy in the Kohn-Sham decomposition (2.8) for this expansion of the density yields the *Kohn-Sham equations*, which are solved iteratively/self-consistently [8, 15].

As the exchange-correlation function $E_{xc}[n(\mathbf{r})]$ is unknown and no systematic procedure for improvement exists, there are a large number of approximations of it. Two important classes are the *local density approximation* (LDA) and *generalized gradient approximation* (GGA). LDAs, still popular in solid-state physics, can be written as[4]

$$E_{xc}^{LDA}[n(\mathbf{r})] = \int f(n(\mathbf{r})) \, d\mathbf{r}. \tag{2.11}$$

GGAs, more commonly used by chemists, introduces a non-local dependence on the gradient of the density $\nabla n(\mathbf{r})$:

$$E_{xc}^{GGA}[n(\mathbf{r})] = \int f(n(\mathbf{r}), \nabla n(\mathbf{r})) \, d\mathbf{r}. \tag{2.12}$$

In our calculations, we have used the B3LYP functional. It is a hybrid functional: the exchange-correlation energy is written as a weighted sum, fitted to atomic data, of the Hartree-Fock exchange, an LDA, and two GGAs [16].

2.4 Basis Sets

The molecular orbitals $\varphi_i(\mathbf{r})$ in equation (2.10) are normally expanded in terms of a *basis set* of *atomic orbitals* $\chi_n(\mathbf{r})$. That is,

$$\varphi_m(\mathbf{r}) = \sum_n c_{mn} \chi_n(\mathbf{r}). \tag{2.13}$$

The problem of minimizing the energy (2.8) thus reduces to determining the coefficients c_{mn}.

In our calculations we have used the 6-31g(d) Pople basis set[5]. Such Pople bases consist of *Gaussian type orbitals* (GTOs),

$$\chi_{i,j,k,\zeta}^{GTO}(\mathbf{r}) = N x^i y^j z^k e^{-\zeta r^2}, \tag{2.14}$$

where N is a normalization factor, i, j, k are integers, and ζ is a constant. Orbitals of high $i + j + k$ and low ζ are often added to typical basis sets; they are called *polarization* (denoted $*$) and *diffuse* (denoted $+$) functions, respectively.

---

[3]This is the form of a density derived from a determinantal wave function (a Slater determinant).

[4]I have chosen to ignore spin; for an introduction to treating spin in DFT, see Jacob and Reiher [15].

[5]Also denoted 6-31g*. Detailed descriptions of this notation can be found elsewhere, e.g. Helgaker et al. [12].

2.5 Nuclear Motion: Translation, Rotation and Vibration

In the Born-Oppenheimer approximation, nuclear and electronic motion are decoupled. Although not an equally good approximation, it is useful to consider the different forms of nuclear motion—translation, rotation, and vibration—as separable as well. If such an approximation is made, the energy of an isolated molecule can be decomposed as

$$E = E_{\text{elec}} + E_{\text{trans}} + E_{\text{rot}} + E_{\text{vib}}. \tag{2.15}$$

Each of these modes of motion has a set of states with different energies. Now consider a gas consisting of many molecules, all having the possibility of being in these different energy states. For such macroscopic systems, thermodynamics provides a description through quantities such as temperature and pressure. How these quantities emerge from the quantum mechanics governing the world of molecules is the subject matter of statistical mechanics, to which we return in Section 2.6.2.

The following section will begin by clarifying some terminology before returning to the issue of treating many-molecule systems; resolving this issue will lead us to the enthalpy of formation.

2.6 The Enthalpy of Formation

2.6.1 The Enthalpy, the Reaction Enthalpy, and the Enthalpy of Formation

Definition 2 *The **enthalpy** H of a system is defined as*

$$H = E + pV, \tag{2.16}$$

where E, p, and V is the energy, pressure, and volume of the system, respectively.

The "reaction enthalpy" is a common term in the literature; however, as one may note from the above definition, talking about the enthalpy as a property of a *reaction* (instead of a *system*) can lead to some confusion. The reaction enthalpy is actually a weighted sum of component enthalpies:

Definition 3 *The **reaction enthalpy** $\Delta_{rx}H$ of a reaction with stoichiometric numbers $\nu_1, \nu_2, \dots, \nu_n$ is defined as*

$$\Delta_{rx}H = \sum_{i=1}^{n} \nu_i H_i, \tag{2.17}$$

where H_i is the enthalpy of the component i.

Finally, we define the enthalpy of formation:

Definition 4 *The **enthalpy of formation** of a molecule, denoted $\Delta_f H$, is defined as the reaction enthalpy of the reaction forming the molecule from its constituent elements in their most stable state at temperature $T = 298$ K and pressure $p = 1$ atm [17].*

The enthalpy of formation of a compound is very important for the performance of high-energy materials; it allows for the calculation of the amount of energy released in decomposition or combustion [18].

2.6.2   The Road from Energies to Enthalpies: Statistical Mechanics

To evaluate the formation enthalpy of a compound we need to be able to find component enthalpies. For this, we apply the standard statistical mechanics procedure[6]: find the energy states E_i; form the partition function

$$\mathcal{Q} = \sum_i g(E_i) \exp(-E_i/kT), \tag{2.18}$$

$g(E_i)$ being the degeracy of E_i; calculate the enthalpy H from $\mathcal{Q}$. In general, the partition function, and hence the enthalpy, is a function of temperature and pressure:

$$\mathcal{Q} = \mathcal{Q}(T, p), \quad H = H(T, p). \tag{2.19}$$

In the case of decoupled electronic, translational, rotational, and vibrational states, the partition functions for each mode of motion forms the molecular partition function

$$\mathscr{Q} = \mathcal{Q}_{\text{elec}} \, \mathcal{Q}_{\text{trans}} \, \mathcal{Q}_{\text{vib}} \, \mathcal{Q}_{\text{rot}} \tag{2.20}$$

resulting in the addition of energies, in accordance with equation 2.15. If one now considers a set of N non-interacting indistinguishable molecules, an ideal gas, the total partition function $\mathcal{Q}$ is obtained by

$$\mathcal{Q} = \frac{\mathscr{Q}^N}{N!}. \tag{2.21}$$

Thus, for an ideal gas, finding $H_i(T, p)$ for the component i amounts to knowing the electronic, translational, vibrational, and rotational energy states. For the modes of motion where all the states are freely available for excitation [20], the *equipartition principle* holds: each degree of freedom contributes

$$\frac{1}{2}RT \tag{2.22}$$

to the energy. We assume this to be true for translational and rotational energy levels. Similarly, we assume that none of the excited electronic states are available; this allows us to consider only the ground state. Vibrational energy levels, however, must be treated explicitly.

2.6.3   Vibrational Motion: The Harmonic Oscillator

Treating vibrational motion is elegantly done by the *harmonic oscillator approximation*, in which the potential $E(\mathbf{R})$ experienced by the nuclei is expanded about an equilibrium geometry

---

[6]Essentially, this amounts to finding the partition function, because every thermodynamic quantity (enthalpy, entropy, internal energy, chemical potential, etc.) can be calculated from it [19].

$\mathbf{R}_{eq}$ to second order (see equation 2.4). If a transformation of the nuclear coordinates $\mathbf{R} \mapsto \mathbf{Q}$ is made, where $\mathbf{Q}$ are called *normal modes*, the wavefunction $\psi_{\text{vib}}(\mathbf{Q})$ takes on a product-form of one-dimensional harmonic oscillators $\psi_{v_i}(Q_i)$ [9]:

$$\psi_{\text{vib}}(\mathbf{Q}) = \prod_i \psi_{v_i}(Q_i) \implies E_{v_1, v_2, \ldots, v_{3N-6}} = \sum_i E_{v_i}. \tag{2.23}$$

With the vibrational energy levels thus found, the partition function $\mathcal{Q}$ can be formed, yielding the final result[7]

$$\begin{aligned}
H(T) &= E(T) + pV \\
&= E(0) + E_{\text{vib}}(0) + E_{\text{vib}}(T) + E_{\text{trans}}(T) + E_{\text{rot}}(T) + RT \\
&= E(0) + \frac{1}{2}h\sum_i f_i + N_A h \sum_i \frac{f_i}{e^{hf_i/kT} - 1} + \frac{3}{2}RT + \frac{3}{2}RT + RT,
\end{aligned} \tag{2.24}$$

where f_i are the vibrational mode frequencies, h is the Planck constant, N_A Avogadro's number, k the Boltzmann constant, and R the universal gas constant. To recap, this is the component enthalpy at temperature T for an ideal gas within the harmonic oscillator approximation. We are actually interested in *solid* formation enthalpies, and one more trick is needed to achieve this: Hess' law.

2.6.4 Hess' Law: Combining Fictitious Reactions

The solid formation enthalpy of a solid $\mathrm{M(s)}$ can in principle be calculated by the same procedure as sketched for an ideal gas above. However, this is a complicated endeavor which we will not pursue. Instead, we take a route through the gas phase by applying the useful Hess' law:

> **Theorem 3 (Hess' Law)** *If $\Delta_{rx}H_i$ are the reaction enthalpies of r reactions, then the reaction enthalpy of the net reaction equals the sum of the individual reaction enthalpies. That is,*

$$\Delta_{rx}H = \sum_{i=1}^{r} \Delta_{rx}H_i. \tag{2.25}$$

Thus we calculate enthalpies for the gas-phase and then apply sublimation enthalpies justified by Hess' law:

$$E(0\,\mathrm{K}, \mathrm{gas}) \xrightarrow{(2.24)} H(T, \mathrm{gas}) \xrightarrow{(\text{Hess' law})} H(T, \mathrm{solid}).$$

As an example, take the compound $C_a H_b N_c O_d(s)$. To apply Hess' law, construct a set of fictitious reactions which, when added all up, result in the formation reaction whose enthalpy of

---

[7]Note that the pressure dependence of H has vanished. This is true for ideal gases [21].

reaction is the enthalpy of formation. One possible choice is the following:

$$a\,C(g) + b\,H(g) + c\,N(g) + d\,O(g) \longrightarrow C_a H_b N_c O_d(g) \tag{2.26}$$

$$C_a H_b N_c O_d(g) \longrightarrow C_a H_b N_c O_d(s). \tag{2.27}$$

$$a\,C(\text{graphite}) \longrightarrow a\,C(g) \tag{2.28}$$

$$\frac{b}{2}\,H_2(g) \longrightarrow b\,H(g) \tag{2.29}$$

$$\frac{c}{2}\,N_2(g) \longrightarrow c\,N(g) \tag{2.30}$$

$$\frac{d}{2}\,O_2(g) \longrightarrow d\,O(g) \tag{2.31}$$
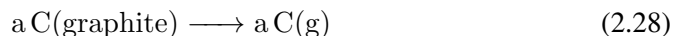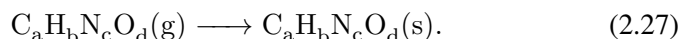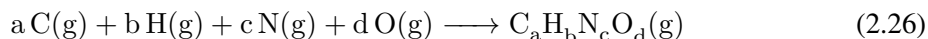
The two cases in which experimental enthalpy data must be used are (2.27) and (2.28). In our work, we used experimental data for (2.27)–(2.31), thus making the following quantum chemical calculations required: energy calculations on C(g), H(g), N(g), O(g), and $C_a H_b N_c O_d$(g).

For the cases in which no enthalpy of sublimation data is available, empirical methods can be used: the *Trouton's approximation* yields the estimate [7]

$$\Delta_{\text{sub}} H[\text{J/mol}] = 188\,T_m[\text{K}], \tag{2.32}$$

where T_m is the melting temperature; if no melting point data is available, the Joback method [22] can first be used for T_m, then (2.32) yields $\Delta_{\text{sub}} H$; and, Keshavarz [23] has published a method for calculating sublimation enthalpies based on molecular weight and some structure contributions.

2.7 Crystal Density Approximations

Detonation and combustion performance depend to a large extent on the crystal density ρ of a compound. Accurate estimation of this quantity is hence crucial to determine whether a novel energetic material is worth pursuing further.

A simple empirical method is the *volume additivity* method. It assigns a certain amount of volume to molecular groups and atoms such that, upon addition of all the individual volume contributions that make up a molecule, we get a "molecular volume". If M is the mass of a single molecule, then the density ρ can be approximated by

$$\rho = \frac{M}{\sum_i V_i}, \tag{2.33}$$

where V_i is the volume contribution of the atom or group i. Holden et al. [24] notes two objections to such an approach: first, the assignment of volume to atoms and groups is, even if one adds the environment of the group as a factor, limited by the scope of the fitting set, and thus is not applicable to novel, unusual compounds; second, it does not readily take into account molecular conformation or crystal packing efficiency.

Rice et al. [1] provided a non-empirical method for calculating the "molecular volume"; they suggested that the volume enclosed by an isosurface of the electron density $n(\mathbf{r})$ provides a

measure of the molecular volume. In particular, they approximated the density by

$$\rho_{\text{isosurface}} = \frac{M}{V}, \tag{2.34}$$

where V is the volume enclosed by the 0.001 electrons/bohr^3 electron density isosurface. Note that this is superior to volume additivity in two respects: there is no fitting to data and it is easily obtained for any molecule. The choice of isosurface is arbitrary, though Rice et al. [1], using the 0.001 electrons/bohr^3 isosurface on 180 neutral CHNO molecules and 38 high-nitrogen molecules, achieved a root-mean-square deviation of 3.6 and 3.4%, respectively.

Although the isosurface method provides a less arbitrary way of predicting the molecular volume, it completely ignores intermolecular interactions. Politzer et al. [2] suggested that information of the intermolecular interactions are present in the electrostatic potential $\mathcal{V}(\mathbf{r})$.

Definition 5 *The **electrostatic potential** (ESP) $\mathcal{V}(\boldsymbol{r})$ of a state with electron density $n(\boldsymbol{r})$ is defined by*

$$\mathcal{V}(\boldsymbol{r}) = \sum_N \frac{Z_N}{|\boldsymbol{R}_N - \boldsymbol{r}|} - \int \frac{n(\boldsymbol{r'})}{|\boldsymbol{r'} - \boldsymbol{r}|} \, d\boldsymbol{r'}, \tag{2.35}$$

where N, Z_N, and $\boldsymbol{R}_N$ denote the nuclei, their atomic numbers, and their position vectors.

Picking one parameter derived from $\mathcal{V}(\mathbf{r})$, restricted to $\mathbf{r}$ on the 0.001 electrons/bohr^3 isosurface, Politzer et al. [2] achieved better agreement with experiment [25]. The parameter considered was

$$\frac{\sigma_+^2 \sigma_-^2}{\sigma_+^2 + \sigma_-^2} \tag{2.36}$$

where σ_-^2 and σ_+^2 are the variances of positive and negative $\mathcal{V}(\mathbf{r})$ values with $\mathbf{r}$ restricted to the isosurface. From this, a least-squares fit was done to

$$\rho_{\text{Politzer}} = \alpha \left(\frac{M}{V} \right) + \beta \left(\frac{\sigma_+^2 \sigma_-^2}{\sigma_+^2 + \sigma_-^2} \right) + \gamma. \tag{2.37}$$

It is important to note that weighting the importance of molecular volume to ESP parameter(s) requires fitting to experimental data, thus bringing back in the empiricism and hence non-transferability.

2.8 Sensitivity

The sensitivity of a material refers to its susceptibility to initiation due to external explosion stimuli. These can be grouped as thermal, mechanical or electrostatic; in particular, common measurements made on explosives include sensitivity to impact, friction, electrostatic discharge, and heat [7].

There is abundant experimental data on impact sensitivity, measured by the so-called drophammer method, thus making it the best candidate for testing theoretical models of sensitivity.

The value measured by drophammer tests is the height h_{50} at which 50% of the drops initiate reaction. Not surprisingly, since the potential energy of a body in a gravitational field is proportional to its mass, the h_{50} value depends on the mass dropped. A measure independent of the mass—at least not in any trivial sense—of the sample is the *impact energy*, defined as [26]

$$I_{50} = mgh_{50}, \qquad (2.38)$$

where g is the acceleration of gravity. This is the kinetic energy at impact for which 50% of the samples dropped initiates.

A large number of correlations between sensitivity and molecular or crystal properties have been identified, including the number of low-frequency (doorway) modes [27, 28], band gaps [29], composition [30], ESP properties [31, 32], and bond dissociation energies [32, 33]. Initiation is a very complex process, as pointed out by Dlott [27], and simple correlation studies should be used with caution as evidence for mechanistic processes. Even so, many of these correlations can be traced to the special properties of $X-NO_2$ bonds, thus leading some to believe the bonds to be "trigger-linkages" for initiation [26].

No matter what the reason, if a correlation exists, it can *predict* the sensitivity of novel compounds for which no data exists. This is our motivation for considering one such correlation: that of bond dissociation energies.

2.8.1 The Bond Dissociation Energy

The work of Mathieu [34] and Song et al. [33] documents a correlation between sensitivity and bond dissosiation energies.

> **Definition 6** *The **bond dissociation energy** (BDE) of a bond, written $A-B$, is defined to be*
>
> $$E_{BDE} = (E(A) + E(B)) - E(A-B), \qquad (2.39)$$
>
> *where $E(X)$ denotes the ground-state electronic energy of compound X (ignoring zero-point vibrational energy).*

In the case of CHNO explosives, the bond(s) in question are of the type $X-NO_2$. If there are several such bonds in a molecule, the one of lowest BDE is used as a measure of sensitivity.

2.8.2 Reaction Kinetics as a Possible Explanation

A possible explanation of the observed correlation of bond dissociation energies and sensitivity is proposed by Mathieu [34]. It is based on Arrhenius kinetics and is described in the following.

Assuming that the rate-limiting step in initiation is the unimolecular dissociation reaction

$$A-NO_2 \longrightarrow [A\cdots NO_2]^{\ddagger} \longrightarrow A\cdot + NO_2\cdot \qquad (2.40)$$
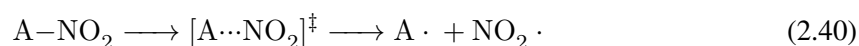
Arrhenius kinetic theory will relate the reaction rate r to the activation energy to reach the transition state $E^\ddagger$ by

$$r = \kappa[\text{A}-\text{NO}_2], \quad \kappa = Ce^{-\frac{E^\ddagger}{RT}}, \tag{2.41}$$

where $[\text{A}-\text{NO}_2]$ denotes the concentration of $\text{A}-\text{NO}_2$ and C is a constant. Taking the logarithm of r, we obtain

$$\ln r = \ln(C[\text{A}-\text{NO}_2]) - \frac{E^\ddagger}{RT}. \tag{2.42}$$

And now comes the key step: we are supposed to believe that the higher the rate of reaction r the higher the sensitivity. That is,

$$\ln\left(\frac{1}{I_{50}}\right) = -\ln I_{50} \propto \ln r = \ln(C[\text{A}-\text{NO}_2]) - \frac{E^\ddagger}{RT}. \tag{2.43}$$

If $\ln(C[\text{A}-\text{NO}_2])$ can be treated as a constant for a set of compounds, then the impact energy can be expressed as

$$\ln I_{50} = C_1\left(\frac{E^\ddagger}{RT}\right) + C_2. \tag{2.44}$$

Initiation in solid explosives is thought to occur by hot-spot formation [35], in which thermal energy become concentrated in small regions of the material. Hence, in such regions, the local temperature T will be very different from the ambient 298 K temperature. The observed correlation of sensitivity to E_{BDE}/E can then be explained if

1. The local temperature is proportional to the energy of the molecule: $T \propto E$.
2. The activation energy is proportional to the bond dissociation energy: $E^\ddagger \propto E_{\text{BDE}}$.

In our work we therefore try to locate transition structures and thus approximate $E^\ddagger$. Based on $T \propto E$,

$$\ln(I_{50}) = C_1'\left(\frac{E^\ddagger}{E}\right) + C_2'. \tag{2.45}$$

Although fewer assumptions are made in (2.45), B3LYP is known to make significant errors in barrier heights [36, 37]. Therefore, we add the second assumption—that is, $E^\ddagger \propto E_{\text{BDE}}$—and postulate that

$$\ln(I_{50}) = C_1''\left(\frac{E_{\text{BDE}}}{E}\right) + C_2''. \tag{2.46}$$

The correlation is not expected to be perfect. First, it ignores the role of the heat capacity and thermal conductivity [26]; if these are high it will help suppress hot-spot formation [27], thus reducing the impact sensitivity. Second, if several weak $\text{X}-\text{NO}_2$ are present, the trigger-linkage hypothesis and simple probability theory dictate that the more such bonds, the more sensitive the compound [34]. Third, the $\text{X}-\text{NO}_2$ bond dissociation might not be the rate-limiting step of initiation.

2.8.3 Complications: Bond Dissociation Energies and Quantum Chemistry

Evaluating the bond dissociation energy (see equation 2.39) requires the calculation of $E(A-NO_2)$, $E(A\cdot)$, and $E(NO_2\cdot)$. Although all these energies are accurate, measured by relative errors, the difference

$$E_{BDE} = (E(A\cdot) + E(NO_2\cdot)) - E(A-NO_2) \qquad (2.47)$$

is a small quantity and may be very inaccurate.

Choosing the same basis set for all three calculations results in an uneven description: the fragments ($A\cdot$ and $NO_2\cdot$) effectively enjoy a larger basis set by "borrowing" from orbitals on the other fragment when part of the molecule $A-NO_2$. This is the *basis set superposition error* (BSSE), which may be corrected for by applying the counterpoise correction [38]. Another source of error is the neglection of zero-point vibrational energies.

In our work neither the BSSE nor zero-point vibrational energies were taken into account. We are encouraged by the fact that, in the work of Song et al. [33], the correlation was equally strong when these effects were taken into account as when they were not.

2.9 Transition Structures

As mentioned in Section 2.1, a transition structure $\mathbf{R}^*$ is a nuclear geometry for which the Hessian $G(\mathbf{R}^*)$ has a single, negative eigenvalue[8].

While minimation runs (i.e. finding equilibrium geometries) usually converge to a minimum irrespective of the suitability of the initial geometry, this is not the case with transition structure searches: for minimization, the gradient always point down-hill; for transition structures, one must step up-hill in one direction and down-hill in every other. Such searches often end in a minimum or a saddle point of order greater than one. Choosing the initial geometry is therefore essential to successfully locate transition structures. There are many possible strategies to choose an initial geometry, and I will review some of them.

One strategy is simply to use "chemical intuition". This corresponds to choosing an initial geometry which minimizes repulsion (according to your own reckoning). A useful assumption to make is the *Hammond postulate*: molecules of similar energy have similar structures [10]. The transition structure is thus more similar to the products in endothermic reactions, and more similar to the reactants in exothermic reactions.

If no analogous reactions exist or intuition fails, there are methods which produce an initial guess for the transition structure from the product and reactant geometries [10]: among these is the *quadratic synchronous transit* (QST) method, in which a series of steps are taken along the path connecting the reactants and product, the maximum being selected as the initial guess; and, the *empirical valence bond* (EVB) model, which constructs surface approximations to the

---

[8]Or a single imaginary frequency, since the frequencies are proportional to the square roots of the eigenvalues [8].

product and reactant minima and look for a minimum along the intersection of the two surfaces.

Another option is to do a *grid search* (or *scan*), in which some coordinates are chosen and $E(\mathbf{R})$ evaluated by incrementally changing these. This can either be done with fixed geometries (*relaxed* search) or re-optimized for each incremental change (*rigid* search).

Once a transition structure search is successful, one must make sure of the following: first, an accurate Hessian must be calculated to confirm the result; second, displacement along the normal mode Q_k corresponding to the negative eigenvalue λ_k must "resemble" the reaction path. If its difficult to ascertain, *reaction path following* should be performed (see Schlegel [10]).

As noted in Section 2.2, methods that perform well for equilibrium geometries and thus for bond dissociation energies (such as B3LYP), may fail to describe transition structures. In particular, B3LYP is known to systematically underestimate barrier heights [36, 37] and inaccurately describe saddle point geometries [37]. Alternative functionals designed to provide accurate saddle point energies; for example, the BH&HLYP (Becke half-and-half LYP), which most significantly differs from B3LYP in that the fraction of Hartree-Fock exchange is increased, performs much better for saddle points [37]. A similar modification of the MPW1PW91, called the modified Perdew-Wang 1-parameter-method (MPW1K), has shown promise [36, 37] and should be considered for future work. Be aware, however, that these modified functionals usually perform worse on equilibrium geometries.

2.10   Detonation and Combustion Parameters

We estimated common performance parameters for a range of CHNO compounds using the EXPLO5 program [39]. For a list of calculated quantities, see Section 3.2.

I will briefly mention the assumptions that are made by the program for calculating the parameters listed above. First, to solve the shock adiabat equation, the phases are modeled by different equations of state (EOS). The gas-phase model is the *Becker-Kistiakowsky-Wilson* (BKW) EOS. For the solid carbon, either the *Cowan and Fickett* EOS or the *Murnaghan* EOS is used. Thermodynamic functions are then calculated using these EOS and the shock adiabat equation solved iteratively yielding the detonation parameters.

To find rocket parameters, such as the specific impulse, the flow through the nozzle must be characterized. The EXPLO5 program allows for the following flow idealizations: *frozen equilibrium*, for which the equilibrium inside the rocket is retained during the flow; *equilibrium flow*, for which the composition is always at chemical equilibrium; or, finally, equilibrium to the nozzle throat and frozen from the throat to the exit. Combining one of the flow idealizations above with the mass, momentum, and energy conservation equations yield the rocket parameters. For these calculations the gas-phase EOS is the *virial equation*, truncated after the ρ^2 term.

3 Procedure

The GAUSSIAN09 software [11] was used for quantum chemical calculations, while the preparation of input files were done in GaussView [40]. For the calculation of detonation and combustion parameters, we used EXPLO5 [39].

3.1 Quantum Chemical Calculations in GAUSSIAN09

Our choice of method was DFT with the B3LYP functional and the 6-31G(d) Pople basis set. To request this method, write `b3lyp/6-31g(d)` in the Route section of the input file.

For geometry optimization, the keyword `opt` is provided in the Route section. To find a transition state instead of a minimum, include the option `ts` in the input: `opt=(ts, calcfc)`. The option `calcfc` ensures that the Hessian is calculated in the initial step.

To find enthalpy corrections, the vibrational energy levels must be calculated. This is done by adding the keyword `freq` in the Route section. To do an optimization and a subsequent vibrational energy calculation, write `opt freq`. The vibrational frequencies also confirm whether a minimum (or transition structure) has been found. The ideal gas enthalpy

$$H(T) = E(T) + RT \tag{3.1}$$

is provided in the output file by e.g.

```
Sum of electronic and thermal Enthalpies=    -878.846571.
```

If the total spin is non-zero an unrestricted formalism must be used. This is requested by adding a "u" in front of the method name, e.g. `ub3lyp`. Below the Route section is a line containing

```
charge   multiplicity
0        2
```

corresponding to a total spin of $1/2$.

GAUSSIAN09 supports the calculation of the electron density and the volume of its 0.001 a.u. isosurface. Requesting the calculation of the density is done by writing `density` in the Route section, while the volume integration by `volume=tight`. The option `tight` is added since the expected accuracy of the Monte carlo integration [41] is only about 10% without it [11].

3.2 Detonation and Combustion Parameters in EXPLO5

In detonation calculations we used the BKWG EOS without covolume corrections. For the combustion parameters, we assumed a chamber pressure of 70 bar and ambient conditions of 1 bar and 298 K as well as equilibrium flow through the nozzle.

Using the crystal density ρ, the heat of formation $\Delta_f H$, and the stoichiometry, the following performance parameters were calculated:

- **Detonation parameters**:
    - Detonation velocity D
    - Detonation pressure P
    - Heat of explosion Q_v
    - Temperature of explosion T_v
    - Specific gas volume released (per mass explosive) V_0

- **Combustion parameters**:
    - Specific impulse I_{sp}.
    - Characteristic exhaust velocity c^*.
    - Combustion chamber temperature T_p.
    - Mean molar mass of gaseous products $\bar{M}_g$.

3.3 Enthalpy of Formation

Calculating the gas enthalpy of formation was done as described in Section 2.6.1. To find the solid enthalpy of formation, the sublimation enthalpy must be subtracted from the gas formation enthalpy by Hess' law. The sublimation enthalpies were estimated by the method described by Keshavarz [23] and by the Trouton method (see equation 2.32). Applying the Trouton method requires the melting point, which was provided by the Joback method [22] if no experimental value was found.

3.4 Crystal Density

In our work, we have estimated the crystal density ρ by the isosurface method suggested by Rice et al. [1] and Politzer et al. [2]. That is, from Rice et al. [1],

$$\rho_{\text{isosurface}} = \frac{M}{V}, \tag{3.2}$$

where V is the volume enclosed by the 0.001 electrons/bohr^3 electron density isosurface. We refer to this as the "isosurface method". Similarly, we refer to the method proposed by Politzer et al. [2],

$$\rho_{\text{Politzer}} = \alpha \left(\frac{M}{V} \right) + \beta \left(\frac{\sigma_+^2 \sigma_-^2}{\sigma_+^2 + \sigma_-^2} \right) + \gamma, \tag{3.3}$$

as the "Politzer method". We used the parameters optimized by Rice and Byrd [25] from 180 neutral and 23 ionic CHNO systems for the B3LYP/6-31g(d,p) level of theory; these are tabulated in Table 3.1. Since the parameters are optimized for 6-31g(d,p) basis set, we recalculated the density with the 6-31g(d,p) basis set (for the 6-31g(d) optimized structures).

Table 3.1 **Optimized Politzer parameters**. *The parameters $\alpha, \beta,$ and γ from [25] optimized to the B3LYP/6-31g(d,p) method and basis set.*

Parameter	Unit	Value
α	g/cm^3	1.0462
β	$g/(cm^3\,E_h{}^2)$	826.8681
γ	g/cm^3	-0.1586

Finding the ESP parameter (given by σ_+ and σ_-) requires the density $n(\mathbf{r})$ (to find the isosurface) as well as the electrostatic potential $\mathcal{V}(\mathbf{r})$ (to calculate the variances). These values can be output from GAUSSIAN09 to so-called CUBE files by using

1. The formchk utility. Creates a formatted checkpoint file (.fch) from the checkpoint file (.chk).
2. The cubegen utility. This creates a CUBE file (.cub) file from the .fch file containing values of the quantity of interest. We chose the default 80^3 points of evaluation. (This, on average, yielded about 2000 points on the 0.001 electrons/bohr^3 isosurface.)

Reading off the data from these .cub files we did with a MATLAB program (see Appendix D). To identify a point as "on" the isosurface, we set the tolerance to

$$\left| n(\mathbf{r}) - 0.001 \text{ electrons/bohr}^3 \right| < 10^{-4} \text{ electrons/bohr}^3. \tag{3.4}$$

3.5 Bond Dissociation Energies

For compounds containing $X-NO_2$ bonds we calculated the dissociation energies by using equation 2.39. If several such bonds were present, we only used the lowest E_{BDE} in the sensitivity correlation.

3.6 Transition structures

Three strategies were used to produce initial geometries for transition structure searches:

1. Intuition. Guessing non-systematically by stretching $X-NO_2$ bonds and changing the $O-N-O$ angle.
2. Hammond's postulate. Weighted averaging of the Z-matrices of the optimized geometries of the reactant, $Y-NO_2$, and the products, $Y\cdot$ and $NO_2\cdot$. For the script used, see Appendix E.
3. Quadratic synchronous transit (QST). The input for such searches was from optimized geometry of reactants and products (QST2) and with an additional Hammond transition state guess (QST3). In GAUSSIAN09 this is requested by adding `opt=QSTn` to the Route section.

Confirming the result was done by recalculating an accurate Hessian (`freq`) and inspecting the normal mode displacement in GaussView5.

4 Results

4.1 Enthalpy of Formation

Gas formation enthalpies, calculated by DFT at the B3LYP/6-31g(d) level of theory, are listed
in Table 4.2. Atomic energies of C, H, N, O, and B was required to find these and are listed in
Appendix A. From the gas formation enthalpies, estimates of the solid formation enthalpies was
obtained by the Keshavarz and Joback/Trouton methods and are listed in Table 4.1. Comparison
of gas and solid formation enthalpies is shown in Figures 4.1 and 4.2.

Table 4.1   **Solid formation enthalpies.** *The formation enthalpies $\Delta_f H_{solid}$ calculated by the
Keshavarz and Joback/Trouton method are listed and compared to experimental values
when possible. Values for which an experimental melting point value was used instead
of the Joback estimate are marked with a dagger* (†).

Compound	$\Delta_f H_{\text{solid}}^{\text{calc}}$ [kJ/mol]		$\Delta_f H_{\text{solid}}^{\text{exp}}$ [kJ/mol]	Deviation [kJ/mol]	
	Keshavarz	Joback/Trouton		Keshavarz	Joback/Trouton
RDX (**1**)	67.8	108.4†	79.1[42]	−11.3	29.3
NTO (**2**)	−35.4	−95.8†	−117.2[43]	81.8	21.4
TNT (**3**)	−32.2	−22.9†	−63.2[44]	31.0	40.3
(**4**)	200.5	175.5†	93.7[3]	106.8	81.8
(**5**)	105.2	36.5	–	–	–
(**6**)	111.8	71.3	–	–	–
(**7**)	137.8	37.5	–	–	–
(**8**)	176.3	104.4	–	–	–
(**9**)	428.4	344.9	372.8[5]	55.6	−27.9
(**10**)	696.3	594.7	667.8[5]	28.5	−73.1
(**11**)	661.6	601.1	673.2[5]	−11.6	−72.1
(**13**)	−579.9	−518.1	–	–	–
(**14**)	633.7	536.8	–	–	–

Table 4.2 **Gas formation enthalpies.** *The formation enthalpies* $\Delta_f H_{gas}$ *calculated by DFT-B3LYP/6-31g(d) are listed and compared to experimental values when possible.*

Compound	$\Delta_f H_{\text{gas}}^{\text{calc}}$ [kJ/mol]	$\Delta_f H_{\text{gas}}^{\text{exp}}$ [kJ/mol]	Deviation[kJ/mol]
RDX (**1**)	198.3	191.6[45]	6.7
NTO (**2**)	6.2	–	–
TNT (**3**)	82.1	24.1[46]	58.0
(**4**)	261.6	–	–
(**5**)	159.2	–	–
(**6**)	221.0	–	–
(**7**)	188.3	–	–
(**8**)	241.1	–	–
(**9**)	504.7	–	–
(**10**)	780.0	–	–
(**11**)	710.2	–	–
(**12**)	−273.2	–	–
(**13**)	−415.8	–	–
(**14**)	686.0	–	–
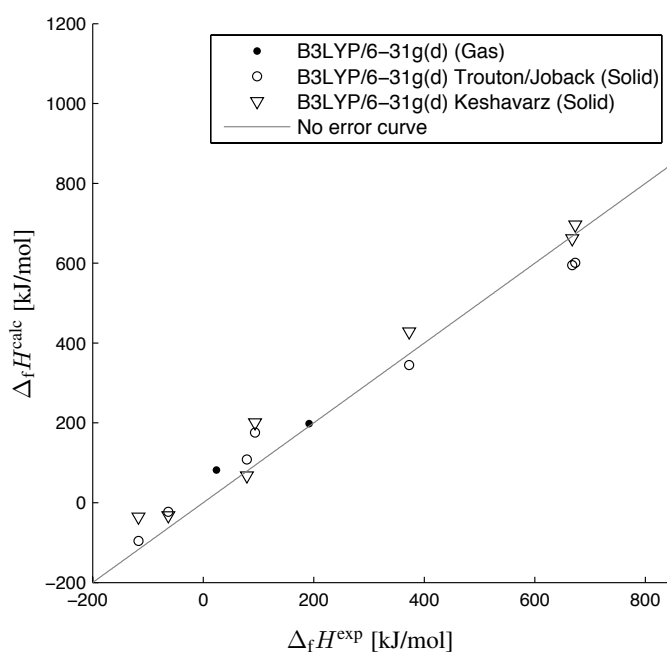
Figure 4.1 **Formation enthalpies as compared to experimental values.** *Calculated gas and solid formation enthalpies* $\Delta_f H^{calc}$ *are plotted against experimental values* $\Delta_f H^{exp}$.
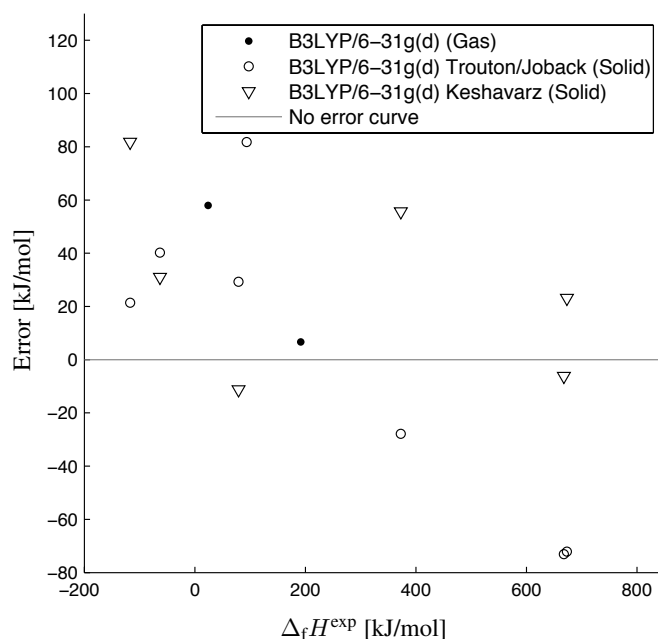
Figure 4.2 **Error of calculated gas and solid formation enthalpies**. *Calculated gas and solid formation enthalpies $\Delta_f H^{calc}$ are plotted against the error compared to experimental values $\Delta_f H^{exp}$.*

4.1.1 Evaluation of the Joback, Trouton, and Keshavarz Methods

Melting points calculated by the Joback group contribution method [22] as well as sublimation enthalpies by the Trouton and Keshavarz method [23] are compared to experimental values in Table 4.4 and 4.3, respectively.

Table 4.3 **Sublimation enthalpies by the Keshavarz and Trouton methods**. *Keshavarz and Trouton sublimation enthalpies are compared to experimental data.*

Compound	$\Delta_{sub}H^{calc}$[kJ/mol]		$\Delta_{sub}H^{exp}$[kJ/mol]	Deviation [kJ/mol]	
	Keshavarz	Trouton		Keshavarz	Trouton
RDX (**1**)	130.4	89.9	112.5[45]	17.9	-22.6
TNT (**3**)	114.3	66.8	105.0[47]	9.3	-38.2

Table 4.4 **Melting points by the Joback method.** *Calculated melting points T_m^{Joback} are compared to experimental data.*

Compound	T_m^{Joback}[K]	T_m^{exp}[K]	Deviation[K]
RDX (**1**)	710.4	478.2	232.2
NTO (**2**)	628.3	542.7	85.6
TNT (**3**)	666.5	355.1	311.4
(**4**)	785.2	458.2	327.0

4.2 Crystal Density

Calculated and experimental crystal densities are presented in Table 4.5 and Figures 4.3, 4.4. The calculated densities was obtained by the Politzer and isosurface methods, as described in 3.4.
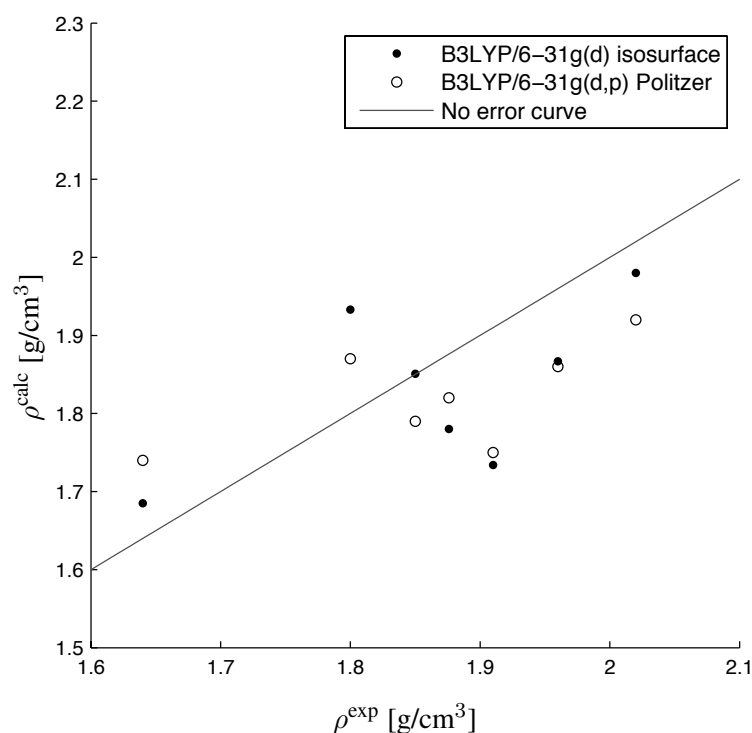
Figure 4.3 **Calculated crystal densities compared with experimental data.** *Calculated densities ρ^{calc} by the isosurface and Politzer methods are compared to experimental values ρ^{exp}.*
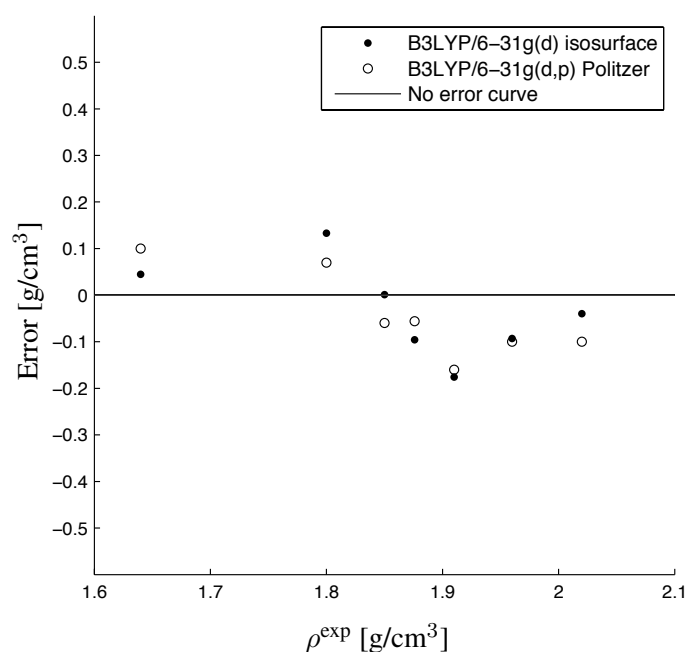
Figure 4.4 **Error of calculated crystal densities**. *Calculated densities ρ^{calc} by the isosurface and Politzer methods are compared to experimental values ρ^{exp} .*

Table 4.5 **Crystal densities**. *Calculated densities ρ^{calc} by DFT-B3LYP: the isosurface method with a 6-31g(d) basis set, and the Politzer method with a 6-31g(d,p) basis set. The calculated densities are compared to experimental data when possible.*

Compound	ρ^{calc}[g/cm^3]		ρ^{exp}[g/cm^3]	Deviation[g/cm^3]	
	Isosurface	Politzer		Isosurface	Politzer
RDX (**1**)	1.93	1.87	1.80[7]	0.13	0.07
NTO (**2**)	1.73	1.75	1.91[48]	-0.18	-0.16
TNT (**3**)	1.69	1.74	1.64[7]	0.05	0.10
(**4**)	1.78	1.82	1.88[3]	-0.10	-0.06
(**5**)	1.85	–	–	–	–
(**6**)	1.92	–	–	–	–
(**7**)	1.87	–	–	–	–
(**8**)	1.83	–	–	–	–
(**9**)	1.87	1.86	1.96[5]	-0.09	-0.11
(**10**)	1.98	1.92	2.02[5]	-0.04	-0.10
(**11**)	1.85	1.79	1.85[5]	0	-0.06
(**12**)	1.59	–	–	–	–
(**13**)	1.82	–	–	–	–
(**14**)	1.84	–	–	–	–

4.3 Detonation and Combustion Parameters

Calculated detonation parameters and combustion parameters are tabulated in Table 4.6 and 4.7, respectively.

Table 4.6 ***Detonation parameters**. Calculated detonation velocity D, detonation pressure P, heat of explosion Q_v, temperature of explosion T_v, and released specific volume V_0. The detonation velocity and pressure was compared to experimental data when possible.*

Compound	D^{calc}[m/s]	D^{exp}[m/s]	P^{calc}[kbar]	P^{exp}[kbar]	Q_v[kJ/kg]	T_v[K]	V_0[m³/mol]
RDX (**1**)	9205	8750[7]	412	347[7]	−6283	4213	731
NTO (**2**)	7633	8560[48]	243	272[48]	−4116	3400	689
TNT (**3**)	7412	6950[7]	230	210[7]	−5382	3743	571
(**4**)	8431	8651[3]	330	359[3]	−6562	5282	638
(**5**)	8387	–	323	–	−5362	4517	672
(**6**)	9192	–	408	–	−6243	4539	748
(**7**)	9017	–	371	–	−5695	3875	776
(**8**)	8389	–	330	–	−6055	4504	632
(**9**)	8703	9600[5]	365	–	−6925	5674	612
(**10**)	9221	10000[5]	428	–	−7106	5734	629
(**11**)	9217	–	406	–	−7388	5996	662
(**13**)	5837	–	137	–	−1562	2078	622
(**14**)	8933	–	355	–	−5711	4370	723

4.4 Statistical Analysis of Methods for Enthalpy, Density, Detonation Velocity and Pressure Estimation

We have calculated root mean square error Δ_{RMSE} and signed mean error Δ_{sgn},

$$\Delta_{\text{RMSE}} = \sqrt{\frac{1}{N} \sum (x_{\text{calc}} - x_{\text{exp}})^2} \tag{4.1}$$

$$\Delta_{\text{sgn}} = \frac{1}{N} \sum (x_{\text{calc}} - x_{\text{exp}}), \tag{4.2}$$

for enthalpies, crystal densities, detonation pressures, and detonation velocities; see Table 4.8.

To find some measure of our ability to distinguish between compounds through our methods, we have considered the approximate 68% confidence interval given by[9] $(\rho - \Delta_{\text{RMSE}}, \rho + \Delta_{\text{RMSE}})$. We define a *confidence interval fraction* ξ as the size of this confidence interval divided by the typical range for the given quantity. It is listed in Table 4.9. If $\xi = 0$, our method is accurate; if $\xi = 1$, we cannot have any confidence in our calculations.

---

[9]This is justified by the fact that Δ_{RMSE} is an estimate for the standard deviation of the error.

Table 4.7 **Combustion parameters**. *Calculated specific impulse I_{sp}, characteristic velocity c^*, isobaric combustion temperature T_p, mean molar mass of gaseous products $\bar{M}_g$, and oxygen balance Ω. In all calculations, the chamber pressure was assumed to be 70 bar and the flow through the nozzle at equilibrium.*

Compound	I_{sp}[s]	c^*[m/s]	T_p[K]	$\bar{M}_g$[g/mol]	Ω[%]
RDX (**1**)	271	1613	3360	24.2	−21.6
NTO (**2**)	211	1309	2399	26.0	−24.6
TNT (**3**)	212	1316	2158	21.6	−74.0
(**4**)	266	2612	3694	30.2	−3.9
(**5**)	250	1410	3378	31.1	4.6
(**6**)	269	1512	3425	27.3	0
(**7**)	258	1569	3035	23.1	−24.5
(**8**)	259	1553	3438	26.6	−25.8
(**9**)	254	1441	3878	31.5	0
(**10**)	261	1475	3961	30.6	0
(**11**)	291	1644	4383	28.3	−10.3
(**13**)	150	924	1617	36.0	35.6
(**14**)	257	1579	3331	24.1	−28.2

4.5 Sensitivity and Bond Dissociation Energy

As expected (see Section 2.8.2) a linear relationship between E_{BDE}/E and $\ln(I_{50}/I_{50}^\circ)$ was obtained,

$$\ln\left(\frac{I_{50}}{I_{50}^\circ}\right) = 1.653 \times 10^4 \left(\frac{E_{\text{BDE}}}{E}\right) + 0.797, \tag{4.3}$$

for the four compounds for which experimental impact sensitivities could be found: RDX (**1**), NTO (**2**), TNT (**3**), and the trinitropyrazole (**4**). The correlation coefficient is $R^2 = 0.9978$ for the logarithmic relationship proposed by Mathieu [34], but only $R^2 = 0.9508$ for the linear relationship proposed by Song et al. [33]. The logarithmic fit is presented in Figure 4.5.

From (4.3) we have estimated the impact sensitivity of the compounds (**5**, **6**, **7**, **8**, **9**, **10**, **12**,

Table 4.8 **Method error estimation**. *The root mean square error and mean signed error, Δ_{RMSE} and Δ_{sgn}, respectively, was found for the methods of enthalpy, density, detonation velocity, and detonation pressure calculation.*

	$\Delta_{\text{f}}H$[kJ/mol]			ρ[g/cm^3]		D[m/s]	P[kbar]
	Joback/Trouton	Keshavarz	DFT (gas)	Isosurface	Politzer		
Δ_{RMSE}	54.7	57.6	41.3	0.10	0.10	676	40
Δ_{sgn}	0	40.1	32.4	−0.03	−0.04	−318	7

Table 4.9 **Confidence interval fraction** ξ. *To calculate this fraction, we have given typical ranges of density, formation enthalpy, detonation pressure, and detonation velocity based on the compounds for which we have experimental data.*

Property	Typical range	Method	Δ_{RMSE}	$\xi = \frac{2\Delta_{\text{RMSE}}}{\text{Typical range}}$
$\Delta_{\text{f}}H$	-200–800 kJ/mol	Joback/Trouton	54.7 kJ/mol	11%
		Keshavarz	57.6 kJ/mol	12%
		DFT (gas)	40.1 kJ/mol	8%
ρ	1.60–2.10 g/cm^3	Isosurface	0.10 g/cm^3	40%
		Politzer	0.10 g/cm^3	40%
D	6500–10000 m/s	Joback/Trouton for $\Delta_{\text{f}}H$, isosurface for ρ, EXPLO5.	676 m/s	38%
P	200–400 kbar	Joback/Trouton for $\Delta_{\text{f}}H$, isosurface for ρ, EXPLO5.	40 kbar	40%

13). The results are summarized in Table 4.10.

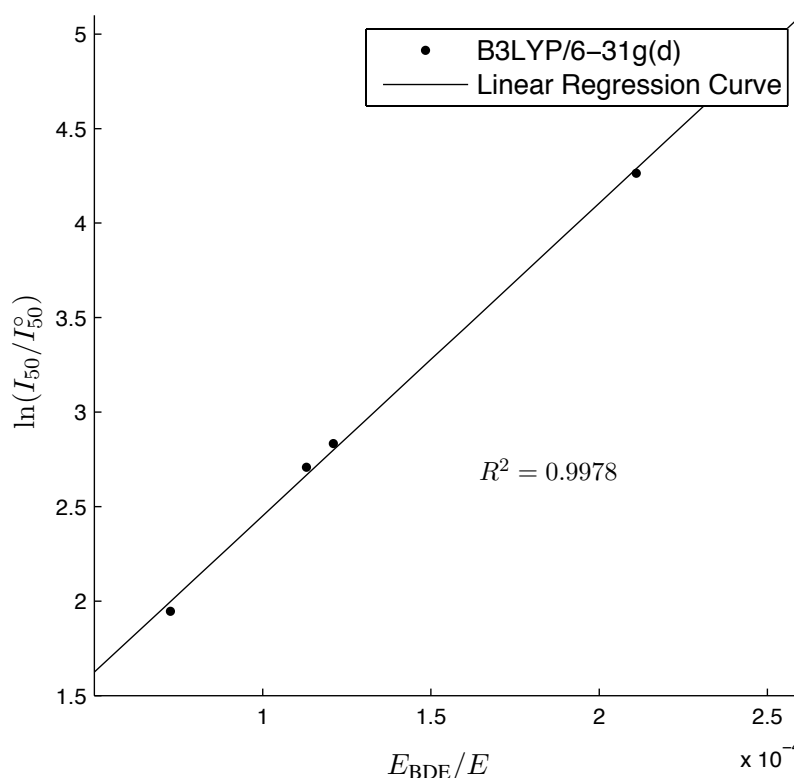*Figure 4.5* **Impact sensitivity correlation with bond dissociation energy**. *Calculated E_{BDE}/E values plotted against the logarithm of experimental impact energies $\ln(I_{50}/I_{50}^{\circ})$, with the impact energy given in J and reference value $I_{50}^{\circ} = 1$ J.*

Using equation 4.3, we estimated the impact sensitivity for the compounds with $X-NO_2$ bonds. These estimates are listed in Table 4.10.

Table 4.10 **Impact energies I_{50} and bond dissociation energies E_{BDE}. Calculated E_{BDE}/E** values for common explosives RDX (**1**), NTO (**2**), TNT (**3**) and the proposed explosives (**4**, **5**, **6**, **7**, **8**, **9**, **10**, **12**, **13**) with $X-NO_2$ bonds. Impact energies have been estimated based on the obtained correlation, see equation (4.3).

Compound	E[kJ/mol]	E_{BDE}[kJ/mol]	E_{BDE}/E	I_{50}^{exp}[J]	I_{50}^{calc}[J]
RDX (**1**)	-2.36×10^6	171.0	7.26×10^{-5}	7[7]	–
NTO (**2**)	-1.37×10^6	289.5	2.11×10^{-4}	71[7]	–
TNT (**3**)	-2.32×10^6	263.5	1.13×10^{-4}	15[7]	–
(**4**)	-2.20×10^6	267.1	1.21×10^{-4}	17[3]	–
(**5**)	-1.91×10^6	45.0	2.36×10^{-5}	–	3.3
(**6**)	-2.25×10^6	43.4	1.93×10^{-5}	–	3.1
(**7**)	-1.72×10^6	211.2	1.23×10^{-4}	–	17.0
(**8**)	-2.31×10^6	266.7	1.16×10^{-4}	–	15.1
(**9**)	-2.84×10^6	120.8	4.25×10^{-5}	–	4.5
(**10**)	-3.13×10^6	81.0	2.59×10^{-5}	–	3.4
(**12**)	-2.25×10^6	204.5	9.10×10^{-5}	–	10.0
(**13**)	-2.07×10^6	121.6	5.88×10^{-5}	–	5.9

4.6 Transition Structures

The initial goal was to find the transition structures for at least RDX (**1**), NTO (**2**), TNT (**3**), and (**4**) to evaluate if

$$E^{\ddagger} \propto E_{\mathrm{BDE}} \tag{4.4}$$

seems to hold for such compounds, but also to see if there existed an impact sensitivity correlation of the form

$$\ln\left(\frac{I_{50}}{I_{50}^{\circ}}\right) = C_1 \left(\frac{E^{\ddagger}}{E}\right) + C_2. \tag{4.5}$$

Locating transition structures turned out be rather difficult. Success was however achieved for NTO (**2**) for which the barrier height was found to be 354.2 kJ/mol with the B3LYP/6-31g(d) method. The geometry of the equilibrium and transition structure is shown in Figure 4.6, and an energy diagram is given in Figure 4.7.

(a) Equilibrium geometry   *(b) Transition structure*
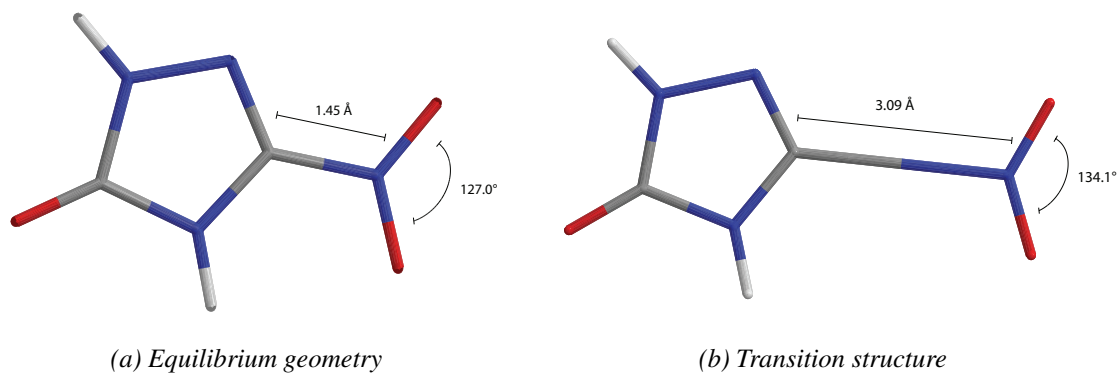
Figure 4.6 **Equilibrium and transition structure geometry of the C$-$NO$_2$ bond dissociation of NTO (2).** *The structures were found by B3LYP/6-31g(d).*
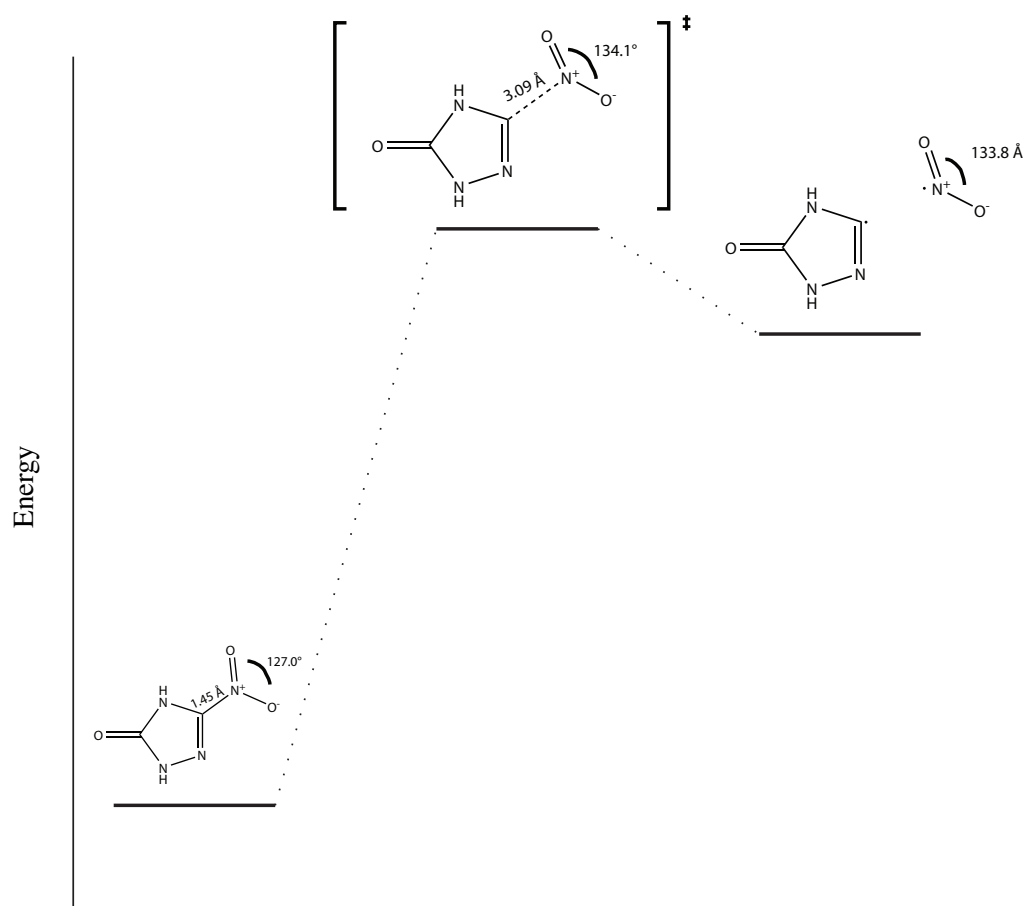

Figure 4.7 **Energy diagram for the C$-$NO$_2$ bond dissociation of NTO (2).** *The structures were all optimized at the B3LYP/6-31g(d) level.*

5 Discussion

5.1 Enthalpy of Formation

The enthalpy of formation $\Delta_f H$ shows a root mean square error of about 55 kJ/mol for both the Joback/Trouton and Keshavarz methods. Given the large range of formation enthalpies, this yields a very good ability to distinguish between compounds ($\xi = 0.11$). We note that all of the estimated enthalpies lie within 105 kJ/mol and half within 50 kJ/mol of the experimental values. Referring to figure 4.2, there is, on average, overestimation for both methods in the range (-200 kJ/mol,+200 kJ/mol). Whether this is a true trend, or a result of the small set of experimental values, should be investigated further. That the Keshavarz method has an signed error of +40.1 kJ/mol reflects this overestimation. A similar underestimation of enthalpies with the Joback method in the (200 kJ/mol, 800 kJ/mol) causes it to have zero signed error.

When comparing the Trouton and Keshavarz methods for obtaining the sublimation enthalpy (Table 4.3) for RDX (**1**) and TNT (**3**), we find that whereas Keshavarz performs well, the Trouton values are underestimates. In addition, as is seen from Table 4.4, the Joback method overestimates the melting point of the compounds (**1**, **2**, **3**, **4**). This combined Joback/Trouton method thus has a fortunate error cancellation: the sublimation enthalpies

$$\Delta_{sub} H^{Joback/Trouton} = 188 T_m^{Joback} \tag{5.1}$$

do seem to have an accuracy comparable to the Keshavarz sublimation enthalpies. The reason for the large errors in Joback melting points is thought to be due to the large $-NO_2$ group contribution of 127 K. In any case, to rely on error cancellation (which may hold for some but not all compounds) is not preferable. We conclude, therefore, that the Keshavarz method is the more reliable and thus the one to use in future work.

5.2 Crystal Density

The success-story of enthalpy of formation is not repeated for the estimation of crystal densities ρ. Our results show a root mean square error of 0.10 g/cm³ for both the isosurface method and the Politzer method, somewhat too high to effectively distinguish between compounds ($\xi = 0.40$). The Politzer method showing similar accuracy is not in agreement with previously reported results [2, 25], but this may be due to too few experimental data points. Further investigations are needed to evaluate which method yield better estimates. However, it may be noted that the worst predictions of the isosurface method (**1**, **2**) are improved in the method of Politzer.

A less optimistic possible conclusion is that the additional parameter of the Politzer method does little or no good. Perhaps other parameters can be suggested that reflect certain situations in which the isosurface method misses the mark. My next step would be to consider the field of crystal structure prediction (CSP) as the best place for ideas; however, CSP is a difficult and ultimately unsolved problem (see Woodley and Catlow [49] for a review).

5.3 The Detonation Velocity and Pressure

The detonation velocity D and pressure P are calculated from $\Delta_\mathrm{f}H$ and ρ, as described in Section 2.10. Thus, in addition to the errors intrinsic to the method of calculation by EXPLO5, the errors in enthalpy and density calculations will contribute. Suspecting that accurate ρ and $\Delta_\mathrm{f}H$ results in accurate D and P, we reran the calculations with experiment density and formation enthalpy. A fourfold reduction in root mean square error for detonation pressure was found, but no improvement for detonation velocity. The reason for this apparent paradox is that the D values of furazan derivatives (**9**, **10**) are underestimated by about 1000 m/s. Since there are no experimental P for these compounds, they do not raise the root mean square error and hence the fourfold decrease. The conclusion to draw is therefore that accurate ρ and $\Delta_\mathrm{f}H$ do result in more accurate performance parameters, but that, for some reason, furazan derivatives are not properly described by the method employed by EXPLO5. The culprit could be the lack of hydrogen in these compounds.

5.4 Sensitivity and Bond Dissociation Energy

Our work on sensitivity correlations were based upon previous work by Mathieu [34] and Song et al. [33]. In the work of Mathieu [34], the correlation

$$\ln\left(\frac{I_{50}}{I_{50}^\circ}\right) = C_1\left(\frac{E_\mathrm{BDE}}{E}\right) + C_2, \tag{5.2}$$

was obtained (but for shock sensitivities, not impact sensitivities). On the other hand, Song et al. [33] obtained a non-logarithmic correlation:

$$I_{50} = C_1\left(\frac{E_\mathrm{BDE}}{E}\right) + C_2. \tag{5.3}$$

These results do not necessarily contradict one another. If a small region of x is considered, the logarithm $\ln(x)$ can appear linear. We included NTO (**2**), which has the remarkably high $I_{50} = 71$ J [7]. Thus, we believe our compounds cover a larger range of sensitivities, and should be better suited to distinguish a logarithmic and linear trend.

Doing a least-squares fit of (5.2) for the compounds (**1**, **2**, **3**, **4**) yielded a correlation coefficient of $R^2 = 0.9978$. A lower correlation coefficient, $R^2 = 0.9508$, was obtained by fitting to (5.3). Our work thus indicates that the logarithmic relationship proposed by Mathieu [34] is more appropriate. The linear and logarithmic fits are shown in Figure 5.1.

The four compounds (**1**, **2**, **3**, **4**) on which the fit was done are very similar to each other and to (**5**, **6**, **7**, **8**, **12**) but very different from the furazan derivates (**9**, **10**, **11**). For this reason, I am less confident in the accuracy of predicted impact energies for (**9**, **10**, **11**).
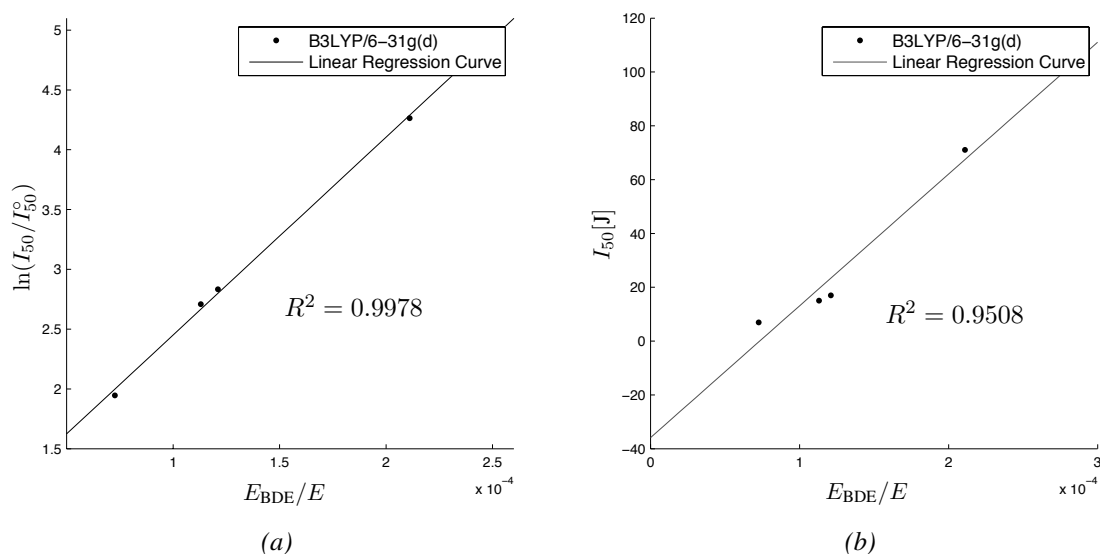
Figure 5.1   **Comparison of linear and logarithmic sensitivity correlation**. *Calculated E_{BDE}/E values are plotted against $\ln(I_{50}/I_{50}^{\circ})$ in (a) and I_{50} in (b). The linear fit to (5.3) and (5.2) are also plotted together with their correlation coefficient R^2.*

5.5 Transition Structures

The approach to transition structures that resulted in the transition structure for NTO (**2**) (see Figure 4.7) was the Hammond postulate approach. The initial guess structure was a weighted average of the Z-matrices of products and reactants: 82% "product-like". The big surprise in the optimized structure is that the $O-N-O$ angle of the transition structure is *larger* than both that of the reactant and product. This might be a recurring pattern in $X-NO_2$ dissociation and initial guesses for other compounds can be chosen with a large $O-N-O$ angle.

The initial purpose of calculating transition structures was to reduce the number of assumptions made in the correlation of bond dissociation energy with impact energy (see Section 2.8.2). Given the correlation found when including the assumption $E^{\ddagger} \propto E_{BDE}$, this original purpose seem less motivated than before. However, the proportionality might not hold in general but only for a certain class of similar compounds, thus making it difficult to accommodate the compounds (**11**, **14**) with no $X-NO_2$ bonds. The obvious and perhaps naive approach is to consider what the first step of decomposition in these compounds is, and then use the bond dissociation energy of this step.

Transition structure searches provide a more powerful approach to reactivity. Proposed reaction mechanisms may be considered by finding their transition structures, and which mechanism dominates can be probed by calculating the energy of these structures. This was indeed done by Tsyshevsky and Kuklja [50] for ANFF-1 and BNFF-1, two compounds similar to the furazan derivatives (**9**, **10**, **11**). Their results indicate that the trigger for initiation is ring-cleavage in these compounds.

5.6 Comparison of Proposed Compounds

Klapötke [7] notes that new nitrogen-rich compounds should not be worse than RDX (**1**) in terms of performance, stability, and chemical properties (low water solubility, smoke-free combustion, etc.). In particular, and relevant to our work, the compound should have the following desired properties:

$$D > 8500 \text{ m/s}$$

$$p > 340 \text{ kbar}$$

$$-Q_v > 6000 \text{ kJ/kg}$$

$$I_{50} > 7 \text{ J}.$$

As discussed in Section 5.3, our ability to distinguish D and p is rather low. Thus, for compounds which have calculated values close to the limits of Klapötke, we cannot say with any certainty whether they have the desired property. On the outset, however, we do have experimental data for some of the compounds: the trinitropyrazole (**4**) satisfies $D > 8500$ m/s and $p > 340$ kbar, while the two furazan derivatives (**10**, **11**) satisfy the velocity requirement. The trinitropyrazole (**4**) also satisfies the sensitivity requirement (17.0 J).

Some calculated values are well above the Klapötke limits, indicating that the corresponding compounds satisfy them; in particular, we note the high detonation velocities and pressures of compounds (**6**, **7**): 9192 m/s, 9017 m/s and 408 kbar, 371 kbar, respectively. While (**6**) is very sensitive (3.1 J), (**7**) has an impact sensitivity comparable to that of TNT (17.0 J). No performance calculations could be done on the boron compound, but we note that its impact sensitivity satisfies the criterion (10.0 J).

The compound studied by FOI (**8**), differing from (**4**) by only a methyl group, does not have improved sensitivity nor detonation nor performance parameters according to our calculations.

Another important performance parameter is the specific impulse. Most compounds has a calculated specific impulse in the range 250–270 s. Those outside this region is NTO (**2**) and TNT (**3**) below (with 211 s and 212 s, respectively) and one furazan derivative (**12**) above (with 291 s). The proposed alternative of NTO with high D, p, and I_{50}, compound (**7**), is in the middle region and hence has a much higher specific impulse (258 s) than that of NTO.

In conclusion, the trinitropyrazole (**4**) and the NTO alternative (**7**) show most promise in this preliminary investigation. Further research is needed to confirm these findings.

6 Conclusions

The impact sensitivity correlation with bond dissociation energy (5.2) reported by Mathieu [34] is in good agreement with our results: the correlation coefficient was found to be $R^2 = 0.9978$ for a set of four common explosives. The linear relationship reported in [33] seem to be due to the small range of sensitivities considered. Our results indicate that there is a correlation for impact sensitivities and not only shock sensitivities, as reported in [34].

For the purposes of accurate performance parameter calculations, the accurate calculation of formation enthalpies and crystal densities is essential. Although there are ways to systematically increase the accuracy of formation enthalpy calculations (which is already reasonably accurate), there is no such procedure for the crystal densities. Although a rough indication of densities can be concluded (into the categories "high" and "low"), many compounds cannot be compared. Further research devoted to correcting the isosurface densities or other approaches (such as CSP) is needed.

Accurate estimation of the important parameters D, P, and I_{sp} depends on accurate ρ, and $\Delta_f H$ calculation. These calculated values thus also falls into rough categories "high" and "low". Nevertheless, they do, by this rough classification, yield a good indication of whether further research and perhaps synthesis of a compound is worth pursuing.

Of the compounds studied, two stand out as promising: The trinitropyrazole (**4**) and (**7**), having high D and p, I_{sp} in the medium range (~ 260 s), and comparable sensitivity to TNT (17.0 J).

7 Epilogue: A Discussion of Crystal Density Corrections

The main conclusion of this report is that crystal density approximations must be improved if true prediction of detonation and performance parameters are to be feasible. Our approach was that of molecular volume V calculated as the interior volume of an isosurface of the electron density $n(\mathbf{r})$. However, if crystal structure prediction is to be avoided, we must make corrections to this approach. The Politzer correction did not improve our predictions to any extent for our set of experimental densities; even so, it may be a reasonable approach to make use of the electrostatic potential $\mathcal{V}(\mathbf{r})$. If electrostatic intermolecular interactions are favorable, this might be reflected in positive and negative values of $\mathcal{V}$ with $\mathbf{r}$ limited to the isosurface.

The issue is then whether the parameter

$$\frac{\sigma_+^2 \sigma_-^2}{\sigma_+^2 + \sigma_-^2} \tag{7.1}$$

adequately describes when corrections to the molecular volume are needed. Politzer argues in the following manner. The quantity

$$\frac{\sigma_+^2 \sigma_-^2}{(\sigma_+^2 + \sigma_-^2)^2} \tag{7.2}$$

has a maximum when both positive and negative regions are equally strong, indicated by $\sigma_+ = \sigma_-$; and, since $\sigma_+^2 + \sigma_-^2$ indicates the strength, the product (7.1) should be large if intermolecular interactions are favorable. Such favorable interactions cause the isosurface method to overestimate the volume and hence underestimate the density. Thus β should be greater than zero in

$$\rho = \alpha \left(\frac{M}{V} \right) + \beta \left(\frac{\sigma_+^2 \sigma_-^2}{\sigma_+^2 + \sigma_-^2} \right) + \gamma. \tag{7.3}$$

The linear correcting of (7.3) means the following: the larger the parameter (7.1) is, the larger the underestimation of ρ. Thus, we should expect a linear decreasing trend if (7.1) is plotted against the error in ρ as calculated by the isosurface method.

Our results does not seem to support a linear decreasing trend, see Figure 7.1. It is unfortunate that we only have seven densities, from which no definite conclusion can be drawn. One may, for example, remove a few presumed "outliers" in Figure 7.1 and achieve a high R^2. However, this results in an increasing trend, contrary to the physical arguments given above.

The choice of the fitting parameters α, β and γ should also be considered. From (7.3) we note that the parameter γ plays the role of correcting for the α scaling of the isosurface density. If we suppose that the extra parameter (7.1) is to play the role of correcting the isosurface estimate, then γ should be dropped altogether and α optimized such that it yields good estimates for compounds with small (7.1).

I propose a somewhat simpler parameter than the one above, but the physical argument is mostly the same. The goal is to find a parameter which is large if interactions are favorable and

small if they are not. The variances σ_-^2 and σ_+^2 certainly reflect if there are negative or positive peaks of $\mathcal{V}(\mathbf{r})$, with $\mathbf{r}$ restricted to the isosurface of $n(\mathbf{r})$. Thus, a simple product form will do: either

$$\sqrt{\sigma_-\sigma_+}, \tag{7.4}$$

the geometric mean of the standard deviations or

$$\sigma_-\sigma_+, \tag{7.5}$$

the geometric mean of the variances. We want the quantity to be significant only when both negative and positive peaks of $\mathcal{V}$ are present, thus the choice of geometric means instead of arithmetic ones.

In Figure 7.2 the quantity $\sigma_-\sigma_+$ is plotted against the error in ρ. One should not read too much into the fact that R^2 is tripled for this choice; there are too few experimental values to compare with to draw any conclusions.
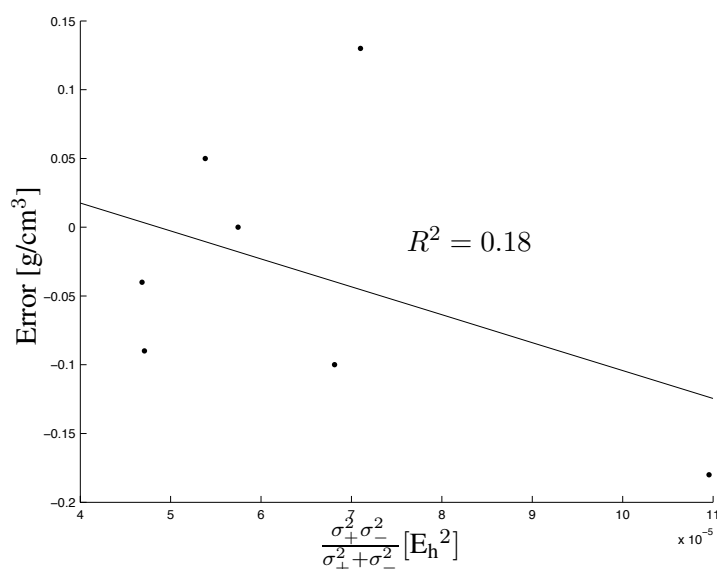

Figure 7.1 **Politzer correction plotted against the error of isosurface densities**. *A linear fit was made, resulting in the correlation coefficient $R^2 = 0.18$.*

The following is an attempt to make precise "favorable intermolecular interactions" and why $\sigma_-\sigma_+$ might be a measure of this. We know that the sign of $\mathcal{V}(\mathbf{r})$ corresponds to a predominance of negative or positive charge in the neighborhood of $\mathbf{r}$. More precisely, it corresponds to the potential energy of a unit point charge due to Coulombic interaction with the nuclei and the electron density $n(\mathbf{r})$. Let positive and negative peaks of the electrostatic potential $\mathcal{V}(\mathbf{r})$ be modeled by point charges q_+ and q_-. Then, if σ_+ and σ_- signify that positive and negative peaks of $\mathcal{V}$ are present, we can identify the product $\sigma_+\sigma_-$ with q_+q_- in an average sense. If we further suppose that intermolecular distances d are similar for different molecules, we find from
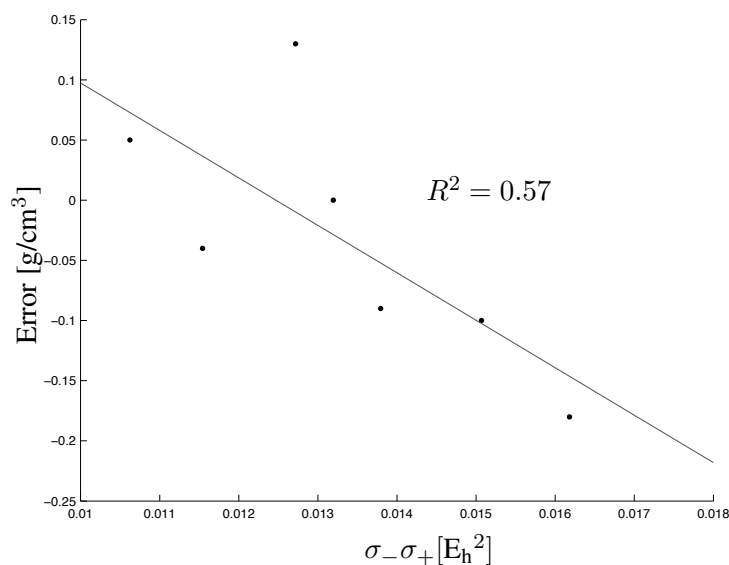
Figure 7.2 **Possible correction factor $\sigma_-\sigma_+$ plotted against the error of isosurface densities**. *A linear fit was made, resulting in the correlation coefficient $R^2 = 0.57$.*

Coulomb's law

$$E_{\text{pot}} \propto \frac{q_+ q_-}{d} \tag{7.6}$$

that the potential energy interaction E_{pot} is roughly measured by the product $\sigma_-\sigma_+$.

Supposing that the isosurface density underestimation is linear in $\sigma_-\sigma_+$, the density ρ can be written

$$\rho = \frac{M}{V} + \beta(\sigma_-\sigma_+). \tag{7.7}$$

This should also include a scaling factor for M/V such that the error is approximately zero when $\sigma_-\sigma_+$ is small. The current V value (by choice of isosurface) is fine-tuned to produce $\Delta_{\text{unsgn}} = 0$. Hence it overestimates the ρ value for compounds with small $\sigma_-\sigma_+$ and overestimate those with large $\sigma_-\sigma_+$. Whether a scaling of the volume $V \mapsto \alpha V$, a constant correction γ for all compounds, or a different isosurface should be chosen is not clear. The form (7.7) is conserved if a new isosurface is chosen; the other two options are

$$\rho = \frac{M}{\alpha V} + \beta(\sigma_-\sigma_+) \tag{7.8}$$

and

$$\rho = \left(\frac{M}{V} + \gamma\right) + \beta(\sigma_-\sigma_+). \tag{7.9}$$

There is little reason, however, to believe that the error in ρ of the isosurface approach is linear in $\sigma_-\sigma_+$. We try to put this on a sounder physical basis. For simplicity, suppose that the

isosurface is a sphere[10] of radius R and that the larger the interaction E_{pot}, measured by $\sigma_-\sigma_+$, the larger the contraction of the sphere. That is, if interaction is included, the radius R contracts by x:

$$R \mapsto R - x, \tag{7.10}$$

where

$$x = \beta(\sigma_-\sigma_+). \tag{7.11}$$

Then we may write the fraction of mass M to volume V as

$$\rho = \frac{M}{\frac{4\pi}{3}(R-x)^3} = \frac{M}{\frac{4\pi}{3}R^3}\left(1 + 3\left(\frac{x}{R}\right) + 6\left(\frac{x}{R}\right)^2 + \ldots\right) \tag{7.12}$$

$$= \rho_0\left(1 + \frac{3\beta}{R}(\sigma_-\sigma_+) + \frac{6\beta^2}{R^2}(\sigma_-\sigma_+)^2 + \ldots\right).$$

where a Taylor expansion about $x = 0$ was done. If only the first-order correction contributes significantly, then we are left with the linear relationship of the correction $\beta(\sigma_-\sigma_+)$:

$$\rho - \rho_0 = \frac{3\beta\rho_0}{R}(\sigma_-\sigma_+). \tag{7.13}$$

Note that this is only strictly true if we can regard ρ_0/R as constant over the set of compounds. Also, this yields us with a simple test: it predicts that the correlation will deteriorate if compounds of very different sizes (R) are considered.

Interested in whether the second-order correction is insignificant, we gave an estimate of β by assuming a first-order correction of the density by 0.10 g/cm^3, a molecular weight of 150 g/mol, and a density of 2 g/cm^3. For this set of values, the second order term is approximately an order of magnitude smaller than that of the first order. That is, the second order correction is about 0.01 g/cm^3 and thus not important to consider.

We note that equation (7.13) indicates that the correction factor should be

$$\sigma_-\sigma_+\left(\frac{\rho_0}{R}\right). \tag{7.14}$$

Whether this improves the correlation is doubtful. The extra factor is a consequence of considering the isosurface to be a sphere, which is certainly not true for most compounds.

The arguments presented here contain a number of assumptions and close agreement with experiment should not be expected. In conclusion, $\sigma_-\sigma_+$ might perform better than (7.1), as suggested by our calculations, but a more extensive set of compounds is needed for a definite answer.

---

[10]A better choice would be an ellipsoid, but this requires more information than the radius R.

References

[1] Betsy M. Rice, Jennifer J. Hare, and Edward F. C. Byrd. Accurate predictions of crystal densities using quantum mechanical molecular volumes. *The Journal of Physical Chemistry A*, 111(42):10874–10879, 2007.

[2] Peter Politzer, Jorge Martinez, Jane S. Murray, Monica C. Concha, and Alejandro Toro-Labbe. An electrostatic interaction correction for improved crystal density prediction. *Molecular Physics*, 107(19):2095–2101, 2009.

[3] Igor Dalinger, Tatyana Pivina, Dmitry Khakimov, Vyacheslav Korolev, and Svyatoslav Shevelev. Trinitropyrazoles: computational stydy of some characteristics.

[4] Stefan Ek. Advances in nitropyrazole chemistry at foi. *New Energetics Workshop. FOI Grindsjön Research Centre, Sweden.*, 2014.

[5] Vitaliy I. Pepekin, Y. N. Matyushin, and Aleksei V. Inozemtsev. Energetic characteristic of furazanotetrazendioxide. *Energetic Materials fEnergetic Materials, Insensitive Munitions and Zero Pollution. 41st International Annual Conference of ICT.*, 2010.

[6] Ernst-Christian Koch and Thomas M. Klapötke. Boron-based high explosives. *Propellants, Explosives, Pyrotechnics*, 37(3):335–344, 2012.

[7] Thomas M. Klapötke. *Chemistry of high-energy materials*. Walter de Gruyter, 2011.

[8] Andrew R. Leach. *Molecular modelling: principles and applications*. Pearson Education, 2001.

[9] Peter Atkins and Ronald Friedman. *Molecular quantum mechanics*. Oxford university press, 2011.

[10] H. Bernhard Schlegel. Geometry optimization. *Wiley Interdisciplinary Reviews: Computational Molecular Science*, 1(5):790–809, 2011.

[11] MJEA Frisch, GW Trucks, Hs B Schlegel, GE Scuseria, MA Robb, JR Cheeseman, G Scalmani, V Barone, B Mennucci, GA Petersson, et al. Gaussian 09, revision a. 02, gaussian. *Inc., Wallingford, CT*, 200, 2009.

[12] Trygve Helgaker, Poul Jørgensen, and Jeppe Olsen. *Molecular electronic-structure theory*. Wiley, 2013.

[13] David Robinson. Splitting multiple bonds: A comparison of methodologies on the accuracy of bond dissociation energies. *Journal of Computational Chemistry*, 34(30):2625–2634, 2013. ISSN 1096-987X. doi: 10.1002/jcc.23433. URL `http://dx.doi.org/10.1002/jcc.23433`.

[14] Pierre Hohenberg and Walter Kohn. Inhomogeneous electron gas. *Physical review*, 136 (3B):B864, 1964.

[15] Christoph R. Jacob and Markus Reiher. Spin in density-functional theory. *International Journal of Quantum Chemistry*, 112(23):3661–3684, 2012.

[16] Axel D. Becke. Perspective: Fifty years of density-functional theory in chemical physics. *The Journal of Chemical Physics*, 140(18): 18A301, 2014. doi: http://dx.doi.org/10.1063/1.4869598. URL `http://scitation.aip.org/content/aip/journal/jcp/140/18/10.1063/1.4869598`.

[17] Peter Atkins and Julio de Paula. *Atkins' physical chemistry*. Oxford University Press, 2014.

[18] Peter Politzer and Jane S. Murray. Energetic materials, part 1. *Detonation, combustion. Elsevier, Amsterdam*, 2003.

[19] Ken A. Dill and Sarina Bromberg. *Molecular driving forces: statistical thermodynamics in chemistry and biology*. Garland Science, 2003.

[20] R. K. Pathria and Paul D. Beale. *Statistical mechanics*. Elsevier, 3rd edition, 2011.

[21] Tore Haug-Warberg. Den termodynamiske arbeidsboken. *Kolofin Forlag AS*, 2006.

[22] Kevin G. Joback and Robert C. Reid. Estimation of pure-component properties from group-contributions. *Chemical Engineering Communications*, 57(1-6):233–243, 1987.

[23] Mohammad H. Keshavarz. Improved prediction of heats of sublimation of energetic compounds using their molecular structure. *Journal of hazardous materials*, 177(1):648–659, 2010.

[24] James R. Holden, Zuyue Du, and Herman L. Ammon. Structure and density predictions for energetic materials. *Theoretical and Computational Chemistry*, 12:185–213, 2003.

[25] Betsy M. Rice and Edward F. C. Byrd. Evaluation of electrostatic descriptors for predicting crystalline density. *Journal of computational chemistry*, 34(25):2146–2151, 2013.

[26] Peter Politzer and Jane S. Murray. Detonation performance and sensitivity: A quest for balance. *Energetic Materials*, 69:1, 2014.

[27] Dana D. Dlott. Fast molecular processes in energetic materials. *Theoretical and computational chemistry*, 13:125–191, 2003.

[28] Ge Su-Hong, Cheng Xin-Lu, Wu Li-Sha, and Yang Xiang-Dong. Correlation between normal mode vibrations and impact sensitivities of some secondary explosives. *Journal of Molecular Structure: THEOCHEM*, 809(1):55–60, 2007.

[29] Hong Zhang, Frankie Cheung, Feng Zhao, and Xin-Lu Cheng. Band gaps and the possible effect on impact sensitivity for some nitro aromatic explosive materials. *International Journal of Quantum Chemistry*, 109(7):1547–1552, 2009.

[30] Mohammad H. Keshavarz. Simple relationship for predicting impact sensitivity of nitroaromatics, nitramines, and nitroaliphatics. *Propellants, Explosives, Pyrotechnics*, 35(2): 175–181, 2010.

[31] Peter Politzer and Jane S. Murray. Sensitivity correlations. *Theoretical and computational chemistry*, 13:5–23, 2003.

[32] Svatopluk Zeman and Zdeněk Friedl. A new approach to the application of molecular surface electrostatic potential in the study of detonation. *Propellants, Explosives, Pyrotechnics*, 37(5):609–613, 2012.

[33] Xiaoshu Song, Xinlu Cheng, Xiangdong Yang, Dehua Li, and Rongfeng Linghu. Correlation between the bond dissociation energies and impact sensitivities in nitramine and polynitro benzoate molecules with polynitro alkyl groupings. *Journal of hazardous materials*, 150(2):317–321, 2008.

[34] D. Mathieu. Theoretical shock sensitivity index for explosives. *The Journal of Physical Chemistry A*, 116(7):1794–1800, 2012.

[35] Qi-Long Yan and Svatopluk Zeman. Theoretical evaluation of sensitivity and thermal stability for high explosives based on quantum chemistry methods: a brief review. *International Journal of Quantum Chemistry*, 113(8):1049–1061, 2013.

[36] Yan Zhao, Núria González-García, and Donald G Truhlar. Benchmark database of barrier heights for heavy atom transfer, nucleophilic substitution, association, and unimolecular reactions and its use to test theoretical methods. *The Journal of Physical Chemistry A*, 109 (9):2012–2018, 2005.

[37] Benjamin J. Lynch and Donald G. Truhlar. How well can hybrid density functional methods predict transition state geometries and barrier heights? *The Journal of Physical Chemistry A*, 105(13):2936–2941, 2001.

[38] C. David Sherrill. Counterpoise correction and basis set superposition error. 2010.

[39] M. Suceska. Explo5. 05 program. *Zagreb, Croatia*, 2011.

[40] Roy Dennington, Todd Keith, and John Millam. Gaussview, version 5. *Semichem Inc., Shawnee Mission KS*, 2009.

[41] Eric W. Weisstein. Monte carlo integration. *From MathWorld, A Wolfram Web Resource. http://mathworld. wolfram. com/MonteCarloIntegratio n. html,(March 18th, 2005)*, 2009.

[42] G. Krien, H. H. Licht, and J. Zierath. Thermochemical investigation of nitramines. *Thermochim. Acta*, 6:465–472, 1973.

[43] Fred Volk and Helmut Bathelt. Influence of energetic materials on the energy-output of gun propellants. *Propellants, explosives, pyrotechnics*, 22(3):120–124, 1997.

[44] Prince E. Rouse Jr. Enthalpies of formation and calculated detonation properties of some thermally stable explosives. *Journal of Chemical and Engineering Data*, 21(1):16–20, 1976.

[45] V. I. Pepekin, Y. N. Matyushin, and Y. A. Lebedev. Thermochemistry of n-nitro-and n-nitrosoamines of the alicyclic series. *Russian Chemical Bulletin*, 23(8):1707–1710, 1974.

[46] Charles Lenchitz, Rodolf W. Velicky, Gayton Silvestro, and Lanny P. Schlosberg. Thermo-dynamic properties of several nitrotoluenes. *The Journal of Chemical Thermodynamics*, 3 (5):689–692, 1971.

[47] Charles Lenchitz and Rodolf W. Velicky. Vapor pressure and heat of sublimation of three nitrotoluenes. *Journal of Chemical and Engineering Data*, 15(3):401–403, 1970.

[48] Matthew W. Smith and Matthew D. Cliff. Nto-based explosive formulations: a technology review. Technical report, DTIC Document, 1999.

[49] Scott M. Woodley and Richard Catlow. Crystal structure prediction from first principles. *Nature materials*, 7(12):937–946, 2008.

[50] Roman V. Tsyshevsky and Maija M. Kuklja. Decomposition mechanisms and kinetics of novel energetic molecules bnff-1 and anff-1: Quantum-chemical modeling. *Molecules*, 18 (7):8500–8517, 2013.

[51] William Clyde Martin and Arlene Musgrove. *Ground levels and ionization energies for the neutral atoms*. NIST Physics Laboratory, 1998.

Appendix A Atomic Energy Calculations

The atomic energy calculations were done at the B3LYP/6-31g(d) level with spin multiplicities of the ground states given by NIST [51]. The results are listed in Table A.1.

Table A.1 **Atomic energy calculations.** *Energies of carbon, hydrogen, nitrogen, oxygen and bohron at the B3LYP/6-31g(d) level are listed.*

Atom	Spin multiplicity ($2S + 1$)	Energy [E_h]
C	3	-37.8462804085
H	2	-0.500272784191
N	4	-54.58448941
O	3	-75.06062312
B	2	-24.6543548367

Appendix B Calculated Politzer Variances

For each compound with experimental crystal densities ρ^{exp}, we found the values σ_- and σ_+ from the ESP $\mathcal{V}$ calculated with the 6-31g(d,p) basis set og 6-31g(d) optimized geometries. The values are listed in Table B.1.

Table B.1 **Calculated variances** σ_-, σ_+. *The variances of the positive and negative regions of $\mathcal{V}$ restricted to the* 0.001 *electrons/bohr^3 isosurface are given for each compound for which experimental density data was available.*

Compound	$\sigma_-[\text{E}_\text{h}]$	$\sigma_+[\text{E}_\text{h}]$
RDX (**1**)	0.0098	0.0165
NTO (**2**)	0.0119	0.0220
TNT (**3**)	0.0091	0.0124
(**4**)	0.0087	0.0261
(**9**)	0.0071	0.0268
(**10**)	0.0074	0.0180
(**11**)	0.0081	0.0215

Appendix C   Calculated Sublimation Enthalpies

Sublimation enthalpies were calculated by the Joback and Keshavarz methods. As the Keshavarz method performed better, the Keshavarz estimates are listed in Table C.1.

Table C.1 **Calculated sublimation enthalpies $\Delta_{sub}H^{Keshavarz}$ by the Keshavarz method.**

Compound	$\Delta_{sub}H^{Keshavarz}$ [kJ/mol]
RDX (**1**)	130.4
NTO (**2**)	41.7
TNT (**3**)	114.3
(**4**)	61.1
(**5**)	53.9
(**6**)	109.2
(**7**)	50.5
(**8**)	64.9
(**9**)	76.3
(**10**)	83.8
(**11**)	48.6
(**12**)	–
(**13**)	164.0
(**14**)	52.3

Appendix D   Processing CUBE files: A MATLAB Script

```matlab
% PROCESSING CUBE FILE TO CALCULATE POLITZER PARAMETERS.
% This script reads the .cub file for both electron density
% and that of the electrostatic potential and pick out values
% on the electrostatic potential limited to the 0.001 au electron
% density surface. Using these points, it calculates the Politzer
% parameters.

ElectronDensityData = importdata('filenameWithElectronicDensity.cub');
ElectrostaticPotentialData = importdata('filenameWithPotential.cub');

% Find which row the listing of points begin (this can probably be
% calculated in some way).
gridPointRowStart = 27;

% First job: find the average positive and average negative
% electrostatic potential value limited to the isosurface.

% We cumulatively add to a vector while counting the number
% of points
numberOfPointsPos = 0;
numberOfPointsNeg = 0;
sumOfElectrostaticPotPos = 0;
sumOfElectrostaticPotNeg = 0;
% The average at the end of the loop will be given by
% numberOfPoints/sumOfElectrostaticPot.

numberOfRows = length(ElectronDensityData.data(:,1));

% Tolerance
tolerance = 0.0001;

for j=1:4
    for i=27:numberOfRows
        % First: is the value in the correct range for the
        % electron density?
        if (isnan(ElectronDensityData.data(i,j)))
            % Do nothing.
        elseif ((abs(ElectronDensityData.data(i,j)-0.001) < tolerance))
            % Check whether the ESP value is negative or positive.
```

```matlab
            if (ElectrostaticPotentialData.data(i,j) < 0)
                numberOfPointsNeg = numberOfPointsNeg + 1;
                sumOfElectrostaticPotNeg = sumOfElectrostaticPotNeg + ...
                    ElectrostaticPotentialData.data(i,j);
            else
                numberOfPointsPos = numberOfPointsPos + 1;
                sumOfElectrostaticPotPos = sumOfElectrostaticPotPos + ...
                    ElectrostaticPotentialData.data(i,j);
            end
        end
    end
end


AveragePositive = sumOfElectrostaticPotPos/numberOfPointsPos;
AverageNegative = sumOfElectrostaticPotNeg/numberOfPointsNeg;

% Now for the variances.

sumOfSquareDevPos = 0;
sumOfSquareDevNeg = 0;

for j=1:4
    for i=27:numberOfRows
        % First: is the value in the correct range
                            % for the electron density?
        if (isnan(ElectronDensityData.data(i,j)))
            % Do nothing.
        elseif ((abs(ElectronDensityData.data(i,j)-0.001) < tolerance))
            % Check whether the ESP value is negative or positive.
            if (ElectrostaticPotentialData.data(i,j) < 0)
                sumOfSquareDevNeg = sumOfSquareDevNeg + ...
                    (ElectrostaticPotentialData.data(i,j)- ...
                    AverageNegative)^2;
            else
                sumOfSquareDevPos = sumOfSquareDevPos + ...
                    (ElectrostaticPotentialData.data(i,j)- ...
                    AveragePositive)^2;
            end
        end
    end
end
```

```matlab
squareDevPos = sumOfSquareDevPos/numberOfPointsPos;
squareDevNeg = sumOfSquareDevNeg/numberOfPointsNeg;

% The parameter Politzer uses is then:
parameter = (squareDevPos*squareDevNeg)/...
    ((squareDevPos + squareDevNeg)^2)*(squareDevPos + squareDevNeg);

% Linear parameters from Rice et al. fitting:
alpha = 1.0462;
beta = 0.0021; % g/cm^3*(1/(kcal/mol)^2) -- convert to hartree/particle!
gamma = -0.1586;

conversionFactor = 627.4924^2; % kcal/mol to hartree/particle in beta.
beta = conversionFactor*beta;

% Calculate the density from the isosurface method (for 6-31G**).
% Fill in values from GAUSSIAN output files.
volume = 110.623; %cm^3/mol
molarWeight = 202.99268; %g/mol
densityIsosurfaceMethod = molarWeight/volume; %g/cm^3

densityPolitzerMethod = alpha*densityIsosurfaceMethod +...
    beta*parameter + gamma;
fprintf('Density (Politzer): %.3f g/cm^3.\n',densityPolitzerMethod);
fprintf('Density (Isosurface): %.3f g/cm^3.\n\n',densityIsosurfaceMethod);
```

Appendix E   Hammond Averaging Z-matrices: A MATLAB Script

This script does not include $NO_2\cdot$ because geometries were optimized for the isolated molecules (not just separated) for bond dissociation energies. A modification of the script is needed if all atoms are present in both Z-matrices.

```matlab
% Script for generating a Z-matrix for initial transition structure guess.
% The values for bond lengths and angles of reactants and
% products are averaged.

% USE HAMMOND'S POSTULATE: in an endothermic process, the transition state
% will be similar to the products. Thus, we weigh the products by a weight
% 0 (pure reactants) -- 1 (pure products).
weight = 0.82;


Molecule = importdata('RDX.txt');
MoleculeWithoutNO2 = importdata('RDXutenNO2.txt');


% WARNING! BEFORE USING SCRIPT: Make sure the connectivity in the
% Z-matrices are identical and do not depend on the group leaving.

% Write the number of atoms in the leaving group:
leavingAtoms = 3; % NO2 group in this case, so 3 atoms.

% The field 'data' of this struct contain the Z-matrix
% in columns 4,5,6.

% Allocate matrix.
numberOfAtoms = length(Molecule.data(:,4));
TransitionStateZMatrix = zeros(numberOfAtoms,3);

% Save the Z-matrices.
MoleculeZMatrix = Molecule.data(:,4:6);
MoleculeWithoutNO2ZMatrix = MoleculeWithoutNO2.data(:,4:6);

% Put NaN logicals in a matrix of same size as TransitionStateZMatrix
% for both.
NaNMolecule = isnan(MoleculeZMatrix);
NaNMoleculeWithoutNO2 = isnan(MoleculeWithoutNO2ZMatrix);
```

```matlab
for j=1:3
    for i=1:numberOfAtoms
        % All but the NO2 values for which there are no matrix elements.
        if (i <= (numberOfAtoms-leavingAtoms))
            if ((NaNMolecule(i,j))||(NaNMoleculeWithoutNO2(i,j)))
                if (NaNMoleculeWithoutNO2(i,j))
                    TransitionStateZMatrix(i,j) = ...
                        MoleculeWithoutNO2ZMatrix(i,j);
                else
                    TransitionStateZMatrix(i,j) = MoleculeZMatrix(i,j);
                end
            else % Average if both values exist.
                TransitionStateZMatrix(i,j) =  ...
                    (1-weight)*MoleculeZMatrix(i,j)+ ...
                    weight*MoleculeWithoutNO2ZMatrix(i,j);
            end
        else
            TransitionStateZMatrix(i,j) = MoleculeZMatrix(i,j);
        end
    end
end

% Print the matrices (and check if they seem reasonable).
fprintf('Input matrices: \n');
disp(MoleculeZMatrix);
disp(MoleculeWithoutNO2ZMatrix);
fprintf('Averaged (weighed!) Z-matrix: \n');
disp(TransitionStateZMatrix);

% Display connection matrix: Needed for writing the Z-matrix for
% the guess structure.

fprintf('Connection matrix: \n');
disp(Molecule.data(:,1:3));

% Also, taking the difference between the products and reactants can reveal
% if some connections are wrong (the differences should be small).

fprintf('Z-matrix for products minus reactants:\n');
disp((MoleculeZMatrix(1:(numberOfAtoms-leavingAtoms), :) -...
    MoleculeWithoutNO2ZMatrix));
```